

Electronic Thesis and Dissertation Repository

2-13-2023 1:00 PM

A Comparison of Methods to Identify the Mean Response Time of Ramp-Incremental Exercise for Exercise Prescription

Nikan Behboodpour, *The University of Western Ontario*

Supervisor: Belfry, Glen R., *The University of Western Ontario*

A thesis submitted in partial fulfillment of the requirements for the Master of Science degree in Kinesiology

© Nikan Behboodpour 2023

Follow this and additional works at: <https://ir.lib.uwo.ca/etd>



Part of the [Exercise Science Commons](#)

Recommended Citation

Behboodpour, Nikan, "A Comparison of Methods to Identify the Mean Response Time of Ramp-Incremental Exercise for Exercise Prescription" (2023). *Electronic Thesis and Dissertation Repository*. 9132.

<https://ir.lib.uwo.ca/etd/9132>

This Dissertation/Thesis is brought to you for free and open access by Scholarship@Western. It has been accepted for inclusion in Electronic Thesis and Dissertation Repository by an authorized administrator of Scholarship@Western. For more information, please contact wlsadmin@uwo.ca.

Abstract

Introduction: The oxygen uptake ($\dot{V}O_2$) vs power output (PO) relationship from ramp incremental exercise (RAMP) is used to prescribe aerobic exercise. As PO increases, there is a delay in $\dot{V}O_2$ that contributes to a misalignment of $\dot{V}O_2$ from PO making precise prescription of exercise PO untenable. Three methods of determining Mean Response Time (exponential modelling (MRT_{EXP}), linear modelling (MRT_{LIN}), and the steady-state method (MRT_{SS})) were compared and evaluated for their accuracy at predicting the $\dot{V}O_2$ associated with two PO below estimated lactate threshold (θ_{LT}) and one above. **Methods:** Ten men performed a $30W \cdot \text{min}^{-1}$ RAMP, and 3-30 min constant PO cycle ergometer trials at the aforementioned intensities. The measured steady-state $\dot{V}O_2$ was compared to the $\dot{V}O_2$ predicted after adjustment by each of the three MRTs. **Results:** For all three MRT methods, predicted $\dot{V}O_2$ was not different ($P=1.000$) from the measured, below θ_{LT} . **Conclusion:** All model predictions can be used for accurate exercise prescription provided the intensity is below θ_{LT} .

Keywords: Time Delay, $\dot{V}O_2$ Kinetics, Constant Power Exercise, Correction Methods, Exercise Intensity Domains

Summary for Lay Audience

Performing a ramp-incremental exercise test (RAMP) is of great benefit as it allows researchers to ascertain physiological variables to prescribe exercise accurately for constant load exercise intensities. The RAMP test also allows us to determine an individual's lactate and respiratory compensation thresholds, which are important in determining their exercise intensity domains (moderate, heavy, severe), all of which are influenced by changes in metabolic pathways and the subsequent cardiorespiratory response to increases in energy demand. However, there is an inherent disconnect between oxygen use by the muscle and the oxygen that is measured through expired air, as blood takes time to reach the lungs and be exhaled at the mouth. This prevents the RAMP from being considered a precise foundation from which to prescribe exercise intensity. There have been three models that account for this delay in order to accurately determine the oxygen use and power output relationship derived from the RAMP test. We investigated these three models in an effort to determine which model is the most accurate at intensities below, slightly below, and slightly above the intensity of work that becomes more challenging. Comparisons were made between an individual's model-adjusted oxygen uptake derived from the RAMP to the oxygen uptake associated with exercise at a known intensity and constant work rate. All three correction methods resulted in a more accurate oxygen uptake to power output relationship during exercise that was easy, however these correction models were not as accurate at predicting the oxygen use at exercise intensities that were harder.

Author Contribution Statement

Nikan Behboodpour (NB), Brayden Halvorson (BH), Juan Murias (JM), Glen Belfry (GB) contributed to the study conception and design. Data collection was performed by NB and BH. Material preparation and analysis were performed by NB. The first draft of the manuscript was written by NB and BH, JM, Daniel Keir (DK) commented on previous versions of the manuscript. All authors read and approved the final manuscript.

Acknowledgements

Firstly, I would like to thank my supervisor, Dr. Glen Belfry. Navigating through the many unique challenges of a graduate program would have been extremely difficult without your valuable advice and support. Thank you for always being a kind and light-hearted soul throughout the process, and someone I could always rely on to get me back on track. Your passion for research and curiosity of the nature of things has left a lifelong impact on my life.

I would also like to thank another source of insight and guidance, Dr. Daniel Keir. Thank you for being a friendly advisor in the lab, and I appreciate your patience in continuously explaining the calculations behind the steady-state MRT method– I finally got it.

I extend my appreciation to my fellow labmates Nasimi Guluzade, Josh Huggard and Jeremy Walsh, for humouring me and playing along in my role of “senior researcher,” good luck in each of your endeavours. To Mustafa Shirzad, Kevin Grossman, and Benjamin Tari – thank you for always being available to help and struggle with me through software and hardware difficulties, you are all great researchers and better friends. To James Van Riesen, Joshua Ahn, and Connor Dalton, thank you for welcoming me into your lab and being a necessary distraction.

To my wonderful partner Saara, thank you for giving me everything I needed throughout this journey, even if I did not know I needed it. Lastly, to my parents, Homa and Mohammad, thank you for being a source of my inspiration throughout my life, I can always count on your love and support through all my efforts.

Table of Contents

Abstract.....	ii
Summary for Lay Audience.....	iii
Author Contribution Statement.....	iv
Acknowledgements.....	v
Table of Contents.....	vi
List of Tables.....	viii
List of Figures.....	ix
List of Abbreviations.....	xi
Chapter 1.....	1
1 « Review of the Literature ».....	1
1.1 « Ramp-Incremental Exercise ».....	2
1.1.1 Energy Systems During RAMP.....	4
1.1.2 Physiological Thresholds during RAMP.....	8
1.1.3 $\dot{V}O_2$ Kinetics during RAMP.....	10
1.2 « Constant-power exercise ».....	11
1.2.1 $\dot{V}O_2$ Kinetics during Constant Power Exercise.....	11
1.3 « Models for determining the MRT ».....	13
1.3.1 Mono-Exponential correction method.....	14
1.3.2 Double-linear correction method.....	15
1.3.3 Steady state correction method.....	16
1.4 « References ».....	18
Chapter 2.....	26
2 « A Comparison of Methods to Identify the Mean Response Time of Ramp-Incremental Exercise for Exercise Prescription ».....	26
2.1 « Introduction ».....	26
2.2 « Methods ».....	28
2.2.2 Data Analysis.....	29
2.2.3 Statistical Analysis.....	31
2.3 « Results ».....	31
2.4 « Discussion ».....	38
2.4.2 MRT Comparisons.....	38
2.4.3 Accuracy of the Prediction Models.....	39
2.4.4 Summary and Conclusion.....	40

2.4.5	Limitations and Future Directions	41
2.5	« References ».....	42
Appendix.....		46
Curriculum Vitae		47

List of Tables

Table 1. Participant characteristics and results from the ramp incremental test (RAMP) (n=10)..... 34

Table 2. Mean response time of the three methods (exponential model; MRT_{EXP} , double-linear model; MRT_{LIN} , and steady-state method; MRT_{SS}) expressed in seconds (s) and Watts (W).....34

Table 3. Mean, SD, and Range of the bias from each predictive method (exponential model; MRT_{EXP} , double-linear model; MRT_{LIN} , and steady-state method; MRT_{SS}) at different intensities.....35

List of Figures

Figure 1. Schematic representation of blood-lactate, ventilatory, and gas-exchange variables: maximum oxygen uptake ($\dot{V}O_{2max}$), ventilation (V_E), end-tidal CO_2 , and end tidal O_2 ($P_{et}CO_2$ and $P_{et}O_2$ respectively) collected during a ramp incremental exercise (RAMP) test. These variables are used to identify estimated lactate threshold, the gas exchange threshold or the first ventilatory threshold (θ_{LT} , GET, or VT_1 respectively), and the respiratory compensation point (RCP) or second ventilatory threshold (VT_2) (Keir et al. 2022)3

Figure 2. ATP-PCr mechanism illustrating the phosphorylation of creatine (Cr) and subsequent adenosine triphosphate (ATP) regeneration. Cytosolic creatine kinase (CK) catalyzes the reaction, transforming phosphocreatine (PCr) in the cytosol to Cr and regenerating adenosine triphosphate (ATP) to be used by the muscle. Mitochondrial creatine kinase (MtCK) catalyzes the reverse reaction using an ATP molecule to regenerate PCr in the mitochondria, which diffuses into the cytosol (Baird et al. 2012)5

Figure 3. Diagram of anaerobic glycolytic pathway in the muscle (di Mauro 2007)6

Figure 4. Illustration of the Electron Transport Chain (ETC), responsible for oxidative phosphorylation (OxPhos) in the mitochondria. Substrates from previous pathways such as the Tricarboxylic Acid (TCA) cycle and/or glycolysis supply electrons to the ETC, creating a proton (H^+) gradient across the inner mitochondrial membrane. This gradient drives the formation of adenosine triphosphate (ATP) through ATP synthase (B. Andrews 2010)8

Figure 5. Example of an individual’s oxygen uptake ($\dot{V}O_2$) kinetics data, organized into the three-phase approach. Phase I, also known as the cardiodynamic component, is a representation of the circulatory transit delay from muscles to the lungs. Phase II represents an exponential increase in $\dot{V}O_2$ due to increased blood flow both to the lungs and skeletal muscle, and subsequently deoxygenated venous blood returning to the lungs. Phase III reflects the achievement of a steady-state $\dot{V}O_2$ in the moderate-intensity domain, or a delayed achievement of a steady-state within the heavy-intensity domain. (McNulty and Robergs 2017)13

Figure 6. Example of the difference between ramp – incremental exercise (RAMP) onset (time = 0) and the intersection of the backwards extrapolation of the oxygen uptake ($\dot{V}O_2$) / time (t) relationship and extrapolation of the baseline $\dot{V}O_2$ to discern the time interval representing this individual’s mean response time (MRT) (Boone and Bourgois 2012a).....16

Figure 7. Example of the difference in power output (PO; measured in Watts, W) between the steady-state $\dot{V}O_2$ (100 W, solid line) and the power output associated with the ramp – incremental (RAMP) $\dot{V}O_2$ (112 W, dotted line). The difference was equivalent to 12 W, which, at a ramp rate of $30W \cdot \text{min}^{-1}$ is 24 seconds (s) and is equivalent to the mean response time (MRT_{SS}) (Iannetta et al. 2019b).....17

Figure 8. Mean Response Time (MRT) values at 75% estimated lactate threshold (θ_{LT}) of a representative individual of the mean response time for an exponential model (A, MRT_{EXP}), the double-linear model (B, MRT_{LIN}), and steady-state method (C, MRT_{SS}; determined using linear interpolation of $\dot{V}O_2$ determined from the three constant load protocols)36

Figure 9. Bar graphs showing mean \pm SD. Lines reflect individual measured and predicted data, of the three models, across three intensities: 75% of lactate threshold (θ_{LT}) (A, D, G, J), 85% θ_{LT} (B, E, H, K) and $\Delta 15\% \theta_{LT} - \dot{V}O_{2\text{max}}$ (15% of the difference between θ_{LT} and $\dot{V}O_{2\text{max}}$) (C, F, I, L). Each graph compared predicted- $\dot{V}O_2$ determined by exponential model (MRT_{EXP}) (A, B, C), linear model (MRT_{LIN}) (D, E, F), steady-state model (MRT_{SS}) (G, H, I), and no model used (NO_{MRT}) (J, K, L) to the actual $\dot{V}O_2$ determined from the last 5 min of each 30 min trial ($\dot{V}O_2$ measured). * Indicates a significant difference of $P < 0.05$37

List of Abbreviations

ADP – Adenosine diphosphate

ANOVA – Analysis of variance

ATP – Adenosine triphosphate

BSL – Baseline

CA – Carbonic anhydrase

CK – Creatine kinase

CO₂ – Carbon dioxide

Cr – Creatine

ETC – Electron transport chain

EXP – Exponential

FAD – Flavin adenine dinucleotide

GET – Gas exchange threshold

H₂O – Water

H⁺ – Hydrogen ion/Proton

HR – Heart rate

La⁻ – Lactate

LIN – Double-linear

min – Minute

MLSS – Maximal lactate steady-state

MRT – Mean response time

NAD – Nicotinamide adenine dinucleotide

NO_{MRT} – no MRT correction model used

OxPhos – Oxidative Phosphorylation

O₂ – Oxygen

PCr -- Phosphocreatine

P_{ET}CO₂ – End-tidal partial pressure of carbon dioxide

P_{ET}O₂ – End-tidal partial pressure of oxygen

PO – Power output

RAMP – Ramp-incremental exercise test

RCP – Respiratory compensation point

RER – Respiratory exchange ratio

S – Second

SS – Steady state

TCA – Tricarboxylic acid

TD – Time delay

V_E – Minute ventilation

$\dot{V}O_2$ – Rate of oxygen uptake

$\dot{V}O_{2m}$ – Skeletal muscle oxygen uptake

$\dot{V}O_{2max}$ – Individual maximum oxygen uptake

$\dot{V}O_{2p}$ – Pulmonary oxygen uptake

$\dot{V}O_{2sc}$ – Slow component

VT_1 – First ventilatory threshold

VT_2 – Second ventilatory threshold

W – Watts

[] – Concentration

θ_L – Lactate threshold

τ – Tau (time constant)

Chapter 1

1 « Review of the Literature »

The ramp-incremental exercise test (RAMP) has become a staple in determining and monitoring important physiological variables such as Gas Exchange Threshold (GET), Respiratory Compensation Point (RCP), maximum oxygen uptake ($\dot{V}O_{2\max}$), ventilation (V_E), end-tidal partial pressure of carbon dioxide, and end tidal partial pressure of oxygen ($P_{et}CO_2$ and $P_{et}O_2$ respectively). Moreover, knowing the power outputs (PO) at which these specific thresholds and associated metabolic and respiratory responses occur, allows researchers, physicians, and trainers alike to provide safe and targeted exercise intensity interventions to improve health and/or athletic performance.

During RAMP, metabolic pathways work in synchrony to meet the energy demands of the continually increasing intensity. These energy demands of the active muscles are met using the anaerobic (without oxygen) and aerobic (with oxygen) energy systems. The two pathways within the anaerobic system are known as the Adenosine Triphosphate–Phosphocreatine (ATP-PCr) and anaerobic glycolytic phosphorylation pathways, the latter using carbohydrates as a substrate exclusively. Oxidative phosphorylation (OxPhos) may use both fats and carbohydrates as substrates. At the onset of ramp incremental exercise, the contributions of these pathways are regulated to provide the necessary energy required to match the demand of the intensity of the exercise. The activation (and subsequent contribution) of each pathway is dependent on exercise intensity (moderate, heavy, severe; these will be further defined below).

As exercise intensity increases in a linear fashion during RAMP, oxygen uptake ($\dot{V}O_2$) also increases in a linear fashion. However, at the onset of RAMP exercise there is an inherent time delay between oxygen uptake per minute ($\dot{V}O_2$) & power output (PO). Without accounting for this time delay, $\dot{V}O_2$ derived from ramp-incremental does not reflect the true $\dot{V}O_2$ for the PO performed. As such, using an “uncorrected” $\dot{V}O_2$ from ramp-incremental exercise results in a lower $\dot{V}O_2$ than is required for that PO. This thesis will elucidate and highlight metabolic and kinetic components that are affected by, and cause, the disconnect that exists between RAMP $\dot{V}O_2$ and

the true $\dot{V}O_2$ performed at a given intensity. Finally, three correction models that have been derived to account for this disconnect, will be discussed. The following section will go through the interplay of metabolism and the cardiorespiratory system as PO increases during RAMP.

1.1 « Ramp-Incremental Exercise »

During RAMP, the increase in exercise intensity causes increasing disturbances to a person's homeostatic levels, reflected by changes in physiological responses (such as $\dot{V}O_2$, $\dot{V}CO_2$, V_E , lactate concentration; $[La^-]$, $P_{et}CO_2$, $P_{et}O_2$, $V_E/\dot{V}CO_2$, $V_E/\dot{V}O_2$, $\dot{V}CO_2/\dot{V}O_2$). These variables can be used to demarcate specific physiological responses that reflect an individual's lactate threshold (θ_{LT}), RCP, and $\dot{V}O_{2max}$. (Figure 1). Until the advent of the ramp incremental test, both a step-incremental test and a constant-power test had to be performed to obtain an individual's physiological parameters (Boone and Bourgois 2012b). Early work suggested that during RAMP, $\dot{V}O_2$ kinetics and power output operate using first-order linear dynamics (Whipp et al. 1981; Boone and Bourgois 2012a) and as such, the change in gas exchange variables could be used to identify an individual's thresholds. Moreover, these physiological thresholds are utilized to distinguish the change in exercise intensity domains: moderate, heavy, and severe (Poole et al. 1988; Caen et al. 2022). During RAMP exercise, the GET (reflecting the lactate threshold), and the RCP are the thresholds that separate these three intensity domains.

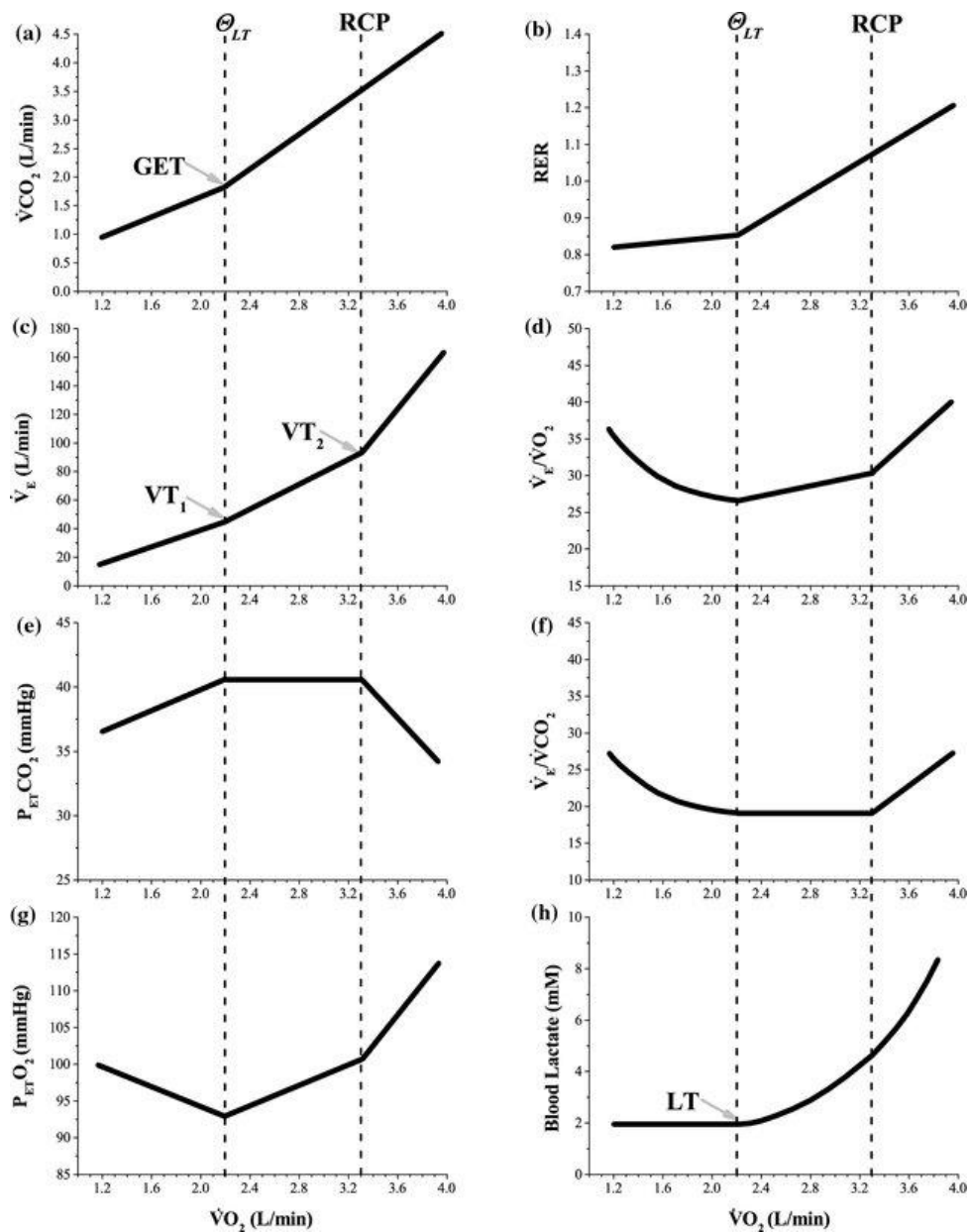


Figure 2. Schematic representation of blood-lactate, ventilatory, and gas-exchange variables: maximum oxygen uptake ($\dot{V}O_{2\max}$), ventilation (V_E), end-tidal CO_2 , and end tidal O_2 ($P_{ET}CO_2$ and $P_{ET}O_2$ respectively) collected during a ramp incremental exercise (RAMP) test. These variables are used to identify estimated lactate threshold, the gas exchange threshold or the first ventilatory threshold (θ_{LT} , GET, or VT_1 respectively), and the respiratory compensation point (RCP) or second ventilatory threshold (VT_2) (Keir et al. 2022).

1.1.1 Energy Systems During RAMP

1.1.1.1 ATP-PCr System

While the ATP-PCr system is known for ATP resynthesis during high-intensity exercise, due to the nature of an incremental test and an inability to indirectly measure the energy derived from the system, its contribution is not considered (Gastin 2001; Bertuzzi et al. 2013). As such, the ATP-PCr system is not a main source of ATP during a ramp-incremental exercise test as the ATP resynthesized from this system is typically used for high-intensity exercise, which requires a demand of up to 5 times greater than that required of a $\dot{V}O_{2\max}$ test (Bertuzzi et al. 2013). Nevertheless, this pathway is involved at the onset of heavy/maximal exercise or during explosive activities when a high rate of energy release is required as the PO demand increases faster than OxPhos can be upregulated during continuous exercise. In this process, mitochondrial ATP transfer a high-energy phosphate to creatine (Cr), forming phosphocreatine (PCr) and adenosine diphosphate (ADP) (Guimarães-Ferreira 2014). PCr then diffuses from mitochondria into the cytoplasm and undergoes a reversible reaction with free-floating cytosolic ADP catalyzed by the creatine kinase (CK) enzyme to regenerate ATP and Cr (Glaister 2005). The ATP is then used for muscle contraction and Cr diffuses back through the mitochondrial membrane (Figure 2). This process does not require any O_2 . During the onset of maximal exercise, [PCr] stores are depleted exponentially, lasting approximately 10 seconds (Glaister 2005). During exercise recovery, resynthesis of PCr occurs primarily by OxPhos and can be described by a monoexponential time course (Arnold et al. 1984; Bendahan et al. 1990; Kemp et al. 1993; Iotti et al. 1993). This recovery period is also independent of exercise intensity, stimulation frequency, and end-levels of PCr (Mahler 1985; Meyer 1988; Thompson et al. 1995). The ATP-PCr system can still be considered a contributor of ATP production as it is estimated to provide between 20-30% of the anaerobic energy during exhaustive exercise lasting 2-3 minutes (Gastin 2001). It is also evidenced by only a ~20% and 50% decrease in [PCr] at moderate and heavy intensities respectively, during constant load (~6min) exercise (Jones et al. 2008). Thus, while the ATP-PCr pathway is not a noticeable contributor during ramp-incremental trials, it is crucial to high-intensity, short duration power outputs, and constant power exercise.

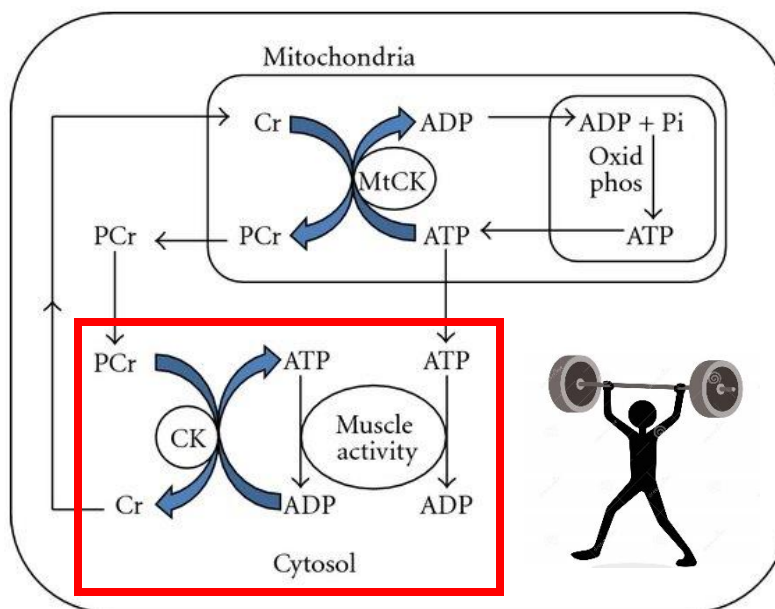


Figure 2. ATP-PCr mechanism illustrating the phosphorylation of creatine (Cr) and subsequent adenosine triphosphate (ATP) regeneration. Cytosolic creatine kinase (CK) catalyzes the reaction, transforming phosphocreatine (PCr) in the cytosol to Cr and regenerating adenosine triphosphate (ATP) to be used by the muscle. Mitochondrial creatine kinase (MtCK) catalyzes the reverse reaction using an ATP molecule to regenerate PCr in the mitochondria, which diffuses into the cytosol (Baird et al. 2012).

Oxidative Phosphorylation and Anaerobic Glycolysis

Throughout the ramp-incremental test, the aerobic pathway (oxidative phosphorylation) remains the main contributor to Adenosine Triphosphate (ATP) regeneration. As exercise intensity increases at a constant predetermined rate in a RAMP, (e.g., 20W/ min, 30 W/min), $\dot{V}O_2$ also increases in a linear fashion following a short delay. At the onset of RAMP and up to GET has been defined as the moderate intensity domain during which OxPhos results in an increase of ATP that matches the increasing energy requirement. To derive this energy from carbohydrates, glycogen and glucose are broken down through a series of reactions (glycolysis) resulting in pyruvate (Figure 3). This molecule then enters one of two energy-producing pathways: anaerobic glycolysis or oxidative phosphorylation. In an absence of/decreased oxygen (O_2) levels in a muscle, or when an ATP demand that is greater than OxPhos, pyruvate will be further catalyzed to lactate. During this process, protons/hydrogen ions (H^+) are produced, simultaneously reducing nicotinamide adenine dinucleotide (NAD^+), an important substrate that can be reused during the

glycolytic pathway (Melkonian and Schury 2022). While this process is inefficient when compared to the ATP yield from oxidative phosphorylation, it phosphorylates ADP approximately 100 times faster (Melkonian and Schury 2022).

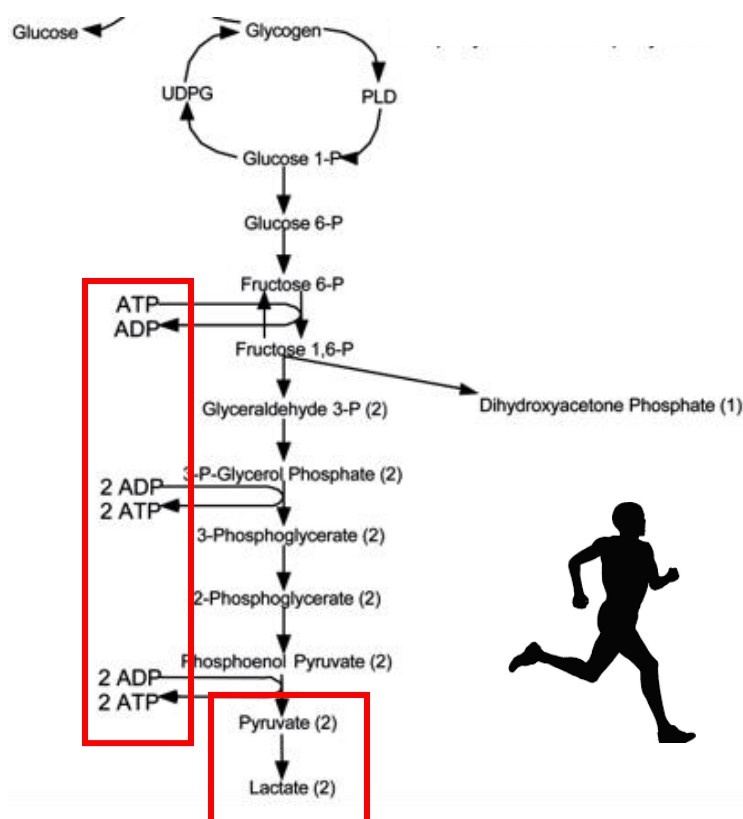


Figure 3. Diagram of anaerobic glycolytic pathway in the muscle (adapted from di Mauro 2007).

However, up to the lactate threshold, pyruvate is mainly shuttled through OxPhos to regenerate ATP from Adenosine Diphosphate (ADP) with the consumption of O_2 . The fuel used to supply this aerobic system is predominantly comprised of carbohydrates and fats. These macronutrients are converted to the required precursors through glycolysis, beta oxidation, and the tricarboxylic acid (TCA) cycle (Nolfi-Donagan et al. 2020). Briefly, pyruvate derived from glycolysis is shuttled into the mitochondria where it is converted into acetyl coenzyme A (Acetyl-CoA), which then enters the tricarboxylic acid (TCA) cycle. Here it is oxidized, helping to reduce NAD^+ to NADH, a necessary coenzyme for the OxPhos pathway (Bartee et al. 2017). NADH is then oxidized by a series of carriers, known together as the electron transport chain (ETC) which simultaneously

pumps the protons (H^+) through a series of complexes that creates an electrochemical gradient across the inner mitochondrial membrane (Figure 4) (Cooper 2000; Xiao et al. 2018; Nolfi-Donagan et al. 2020). This gradient drives the phosphorylation of ADP, where oxygen (O_2) is the final electron acceptor, resulting in the formation of ATP and water (H_2O). Thus, this system only operates in cells that have mitochondria, and available O_2 .

The OxPhos system is the main contributor to ATP regeneration during longer duration exercise because it yields ~36 ATP per glucose molecule versus a net of two ATP regenerated by anaerobic glycolysis (Chaudhry and Varacallo 2022) and conserves carbohydrates and prolongs the possible exercise duration. Moreover, at moderate intensities after the initial $\dot{V}O_2$ kinetic phase the ATP demand can be met exclusively by OxPhos. In the moderate intensity domain, fat oxidation is at its peak, at approximately 60-65% $\dot{V}O_{2max}$, decreasing thereafter (Muscella et al. 2020). To use these fats, or lipids, as an energy source, triacylglycerol (the stored form of fat; TAG) undergoes lipolysis, which separates three fatty acid (FA) chains from a glycerol backbone. First, the glycerol backbone undergoes a series of reactions and enters the glycolytic pathway (Jin et al. 2013). Next, the fatty acid chains undergo a process named beta-oxidation, whereby H^+ ions are removed from them in a cyclical process, generating many acetyl-CoAs as well as reducing NAD and FAD. These H^+ carriers facilitate H^+ entering the electron transfer chain (Purdom et al. 2018). During exercise, proteins are used sparingly as an energy source (unless other sources are not available, or there are excess amino acids present) as they can be broken down into their constituent amino acids and for entry into the TCA cycle at different points, depending on their chemical structure (Bartee et al. 2017).

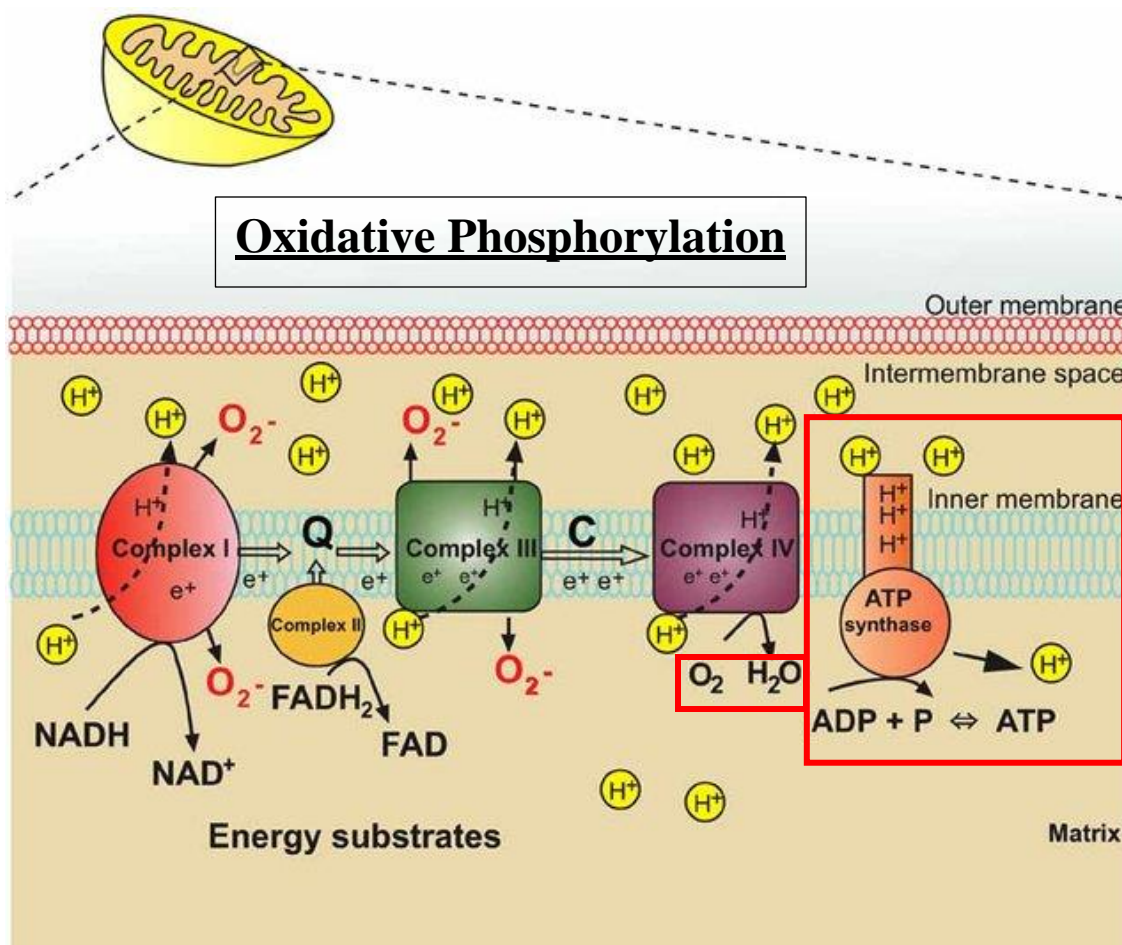


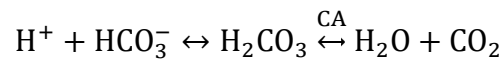
Figure 4. Illustration of the Electron Transport Chain (ETC), responsible for oxidative phosphorylation (OxPhos) in the mitochondria. Substrates from previous pathways such as the Tricarboxylic Acid (TCA) cycle and/or glycolysis supply electrons to the ETC, creating a proton (H^+) gradient across the inner mitochondrial membrane. This gradient drives the formation of adenosine triphosphate (ATP) through ATP synthase (adapted from Andrews 2010).

1.1.2 Physiological Thresholds during RAMP

As exercise intensity increases within the moderate intensity domain, OxPhos will provide nearly all the ATP requirement. Moreover, as an individual continues exercising through this domain, they arrive at the first physiological boundary known as the lactate threshold (θ_{LT}), as determined using ventilatory measures reflecting changes in concomitant respiratory variables that separate the moderate and heavy intensity domain. This point has also been demarcated as the first ventilatory threshold (VT_1), θ_{LT} , or GET (MacIntosh et al. 2021). The GET represents the highest metabolic rate possible without an increase in muscle and blood $[La^-]$ and a subsequent increase

in ventilation. After this point, there is an increase in $\dot{V}CO_2$ to $\dot{V}O_2$ production, resulting in V_E increasing relative to $\dot{V}O_2$, but remains proportional with $\dot{V}CO_2$ (Wasserman et al. 1973; Cerezuela-Espejo et al. 2018; MacIntosh et al. 2021; Keir et al. 2022). The θ_{LT} represents the point at which blood lactate begins to rise (Beaver et al. 1985; MacIntosh et al. 2021). As such, these two concepts (GET and θ_{LT}) are related and can be considered alternatives of one another (Pallarés et al. 2016).

Exercise in the heavy intensity domain results in an upregulation of the pyruvate to lactic acid reaction. This results in an increase in H^+ as lactic acid dissociates immediately upon its formation into lactate and H^+ . This increase in H^+ and the concurrent rise of lactate⁻ to maintain electrochemical neutrality in the muscle and blood from anaerobic glycolysis is buffered by the reversible carbonic anhydrase (CA) reaction that combines bicarbonate and H^+ to form carbon dioxide (CO_2) and H_2O (see below) (Wasserman et al. 1986):



Above the lactate threshold this buffer system is no longer able to keep the accumulating H^+ at near resting levels, and as a result, an increase in [La⁻] is observed. As an individual enters this heavy intensity domain during RAMP, a phenomenon known as the “ $\dot{V}O_2$ slow component” ($\dot{V}O_{2sc}$) develops. This is a disproportional increase in $\dot{V}O_2$, relative to the increase in PO. This non-linear increase in $\dot{V}O_2$ relative to PO has been coined the $\dot{V}O_2$ gain (i.e., $\Delta\dot{V}O_2/\Delta PO$) (Barstow and Mole 1991; Özyener et al. 2001; Keir et al. 2018). However, within RAMP exercise, the $\dot{V}O_{2sc}$ offsets the $\dot{V}O_2$ gain and $\dot{V}O_2$ continues to rise in a linear fashion. This linear $\dot{V}O_2$ response above lactate threshold leads to a misinterpretation of the $\dot{V}O_2$ cost at a given PO relationship during RAMP exercise.

As we approach the upper boundary of the heavy-intensity domain, we arrive at the second threshold marking the beginning of the severe-intensity domain as presented by Keir et al. 2022. This threshold is typically referred to as the second ventilatory threshold (VT_2) or the respiratory compensation point (RCP). At metabolic rates above this threshold (severe intensity), homeostasis is compromised at an exponential rate and is reflected with H^+ accumulation that is associated with the depletion of bicarbonate. This reduces the expiration of CO_2 , termed ventilatory buffering,

which is essential to facilitate the removal of CO₂ and acid base balance (Wasserman et al. 1973; Keir et al. 2022). As such, the RCP reflects the highest metabolic rate that can be maintained without major disruption to the body's internal environment. The $\dot{V}O_2$ at RCP has also been linked to the maximal lactate steady-state (MLSS) and critical power (CP). However, when identifying the PO at which RCP occurs, these surrogates should not be considered equivalent (Iannetta et al. 2020b; Keir et al. 2022). This difference in equivalency can be attributed to the non-linear nature of $\dot{V}O_2$ when performing ramp-incremental exercise. During exercise in the severe intensity domain, above RCP, a disproportional increase in V_E compared to $\dot{V}CO_2$, accompanied with a drop in PCO₂ is observed (MacIntosh et al. 2021). Moreover, as $\dot{V}O_2$ continues to rise, the upper boundary of the severe intensity domain is $\dot{V}O_{2max}$. It is at this level that anaerobic glycolysis becomes a noticeable energy contributor as well (Colosio et al. 2020). However, despite becoming a greater energy contributor above this threshold, anaerobic glycolysis is still not the predominant ATP provider. Rather, at every PO above VT₂ to $\dot{V}O_{2max}$, the primary energy contributor remains OxPhos. It is only at intensities much greater than an individual's $\dot{V}O_{2max}$ (e.g., 150% of $\dot{V}O_{2max}$) that the anaerobic pathway becomes a main contributor (Jones et al. 2008).

1.1.3 $\dot{V}O_2$ Kinetics during RAMP

Since direct measurement of muscle oxygen uptake kinetics ($\dot{V}O_{2m}$) is not easily attainable or feasible during exercise testing, $\dot{V}O_2$ measured at the mouth ($\dot{V}O_{2p}$), representing pulmonary oxygen uptake, is considered an appropriate substitute (Whipp and Ward 1990; Grassi 2000; Jones and Poole 2005). However, when taking into consideration the $\dot{V}O_2$ as measured at the mouth at a specific PO, it is essential to be mindful of the delay between $\dot{V}O_{2m}$ and the $\dot{V}O_{2p}$, as the transit time of deoxygenated blood from the muscle to the lungs is significant. This delay is known as the mean response time (MRT). Above the GET, the presence of the $\dot{V}O_{2sc}$ increases the time it takes $\dot{V}O_2$ to reach a theoretical steady state (which is only visible during constant power exercise) and increases the gain. This leads to a lengthening of the MRT past this threshold, and it is imperative to be mindful of additional adjustments to ensure an accurate relationship between $\dot{V}O_2$ and PO is maintained. The concept of MRT will be further expanded on below.

1.2 « Constant-power exercise »

Performing a constant power exercise test is critical when ascertaining one's $\dot{V}O_2$ at a particular PO. In the present study, participants underwent three separate exercise transitions from rest to a constant power output: two in the moderate intensity domain (75% and 85% GET, respectively) and one in the heavy intensity domain (15% of the difference between GET and $\dot{V}O_{2max}$). Capillary blood samples were used to assess blood [La-] levels to confirm that individuals were exercising within the appropriate exercise intensity domain during the constant power exercise trials. These thresholds and variables are an important part of prescribing individualized and appropriate exercise. During constant power exercise at intensities above θ_{LT} (i.e., going from rest to heavy intensity), a greater reliance on anaerobic metabolism and the aforementioned evolution of the $\dot{V}O_{2sc}$ results in an underestimation of the actual $\dot{V}O_2$ for that PO if observed during RAMP exercise (Grassi 2005; Colosio et al. 2020). At the onset of constant power exercise at all intensities below $\dot{V}O_{2max}$, the anaerobic pathways supply a significant energy requirement for the first 1-2 minutes (McMahon and Jenkins 2002). The delay of this system can be partially attributed to the anaerobic pathways, as they slow the OxPhos regeneration of ATP and the accumulation of ADP (Grassi 2005). This is important as increased [ADP] drives the OxPhos pathway. Moreover, the inherent delay of O₂ delivery to active muscles (Grassi 2005) creates a temporary decrease in its availability, delaying the upregulation of OxPhos (Murias et al. 2014; Colosio et al. 2020). Thus, during moderate and eventually during heavy-intensity constant power exercise, $\dot{V}O_2$ will approach a steady state, however as previously mentioned, the heavy-intensity exercise will display the emergence of the $\dot{V}O_2$ slow component (Korzeniewski and Zoladz 2015).

1.2.1 $\dot{V}O_2$ Kinetics during Constant Power Exercise

As previously established, the transition from rest to a PO of greater intensity creates an increased demand for ATP in the muscle. The longer the exercise modality is maintained, the greater the contribution from OxPhos. To accommodate this increase in activity from this system, $\dot{V}O_2$ increases until it reaches a point where ATP supply matches the ATP demand. This point is known as the steady-state $\dot{V}O_2$. The most widely used model for $\dot{V}O_2$ kinetics during constant power exercise observes a step-increase and has been quantified utilising a three-phase model to predict

$\dot{V}O_2$ adjustments to an increased power output (Figure 5) (Whipp et al. 1982). The first phase (Phase I, also known as the cardiodynamic component) is a representation of the circulatory transit delay from muscles to the lungs (Murias et al. 2011); it is related to increased blood flow to the lungs and is not a representation of skeletal muscle activity in response to exercise (Barstow et al. 1990; Gløersen et al. 2022). The second phase (Phase II) represents an exponential increase in $\dot{V}O_2$ as a result of increased blood flow both to the lungs and skeletal muscle, and subsequently deoxygenated venous blood returning to the lungs (Murias et al. 2011). This phase is also modeled by an exponential component that is arriving at an eventual predicted steady-state (Whipp et al. 1981; Barstow et al. 1990). Lastly, Phase III reflects the achievement of a steady-state $\dot{V}O_2$ in the moderate-intensity domain, or a delayed achievement of a steady-state within the heavy-intensity domain (Murias et al. 2011; Gløersen et al. 2022). The delayed achievement of steady-state $\dot{V}O_2$ is due to the emergence of the $\dot{V}O_{2sc}$. With the presence of this component, the eventual steady-state $\dot{V}O_2$ that is reached will have a greater value than that predicted by a $\dot{V}O_2$ vs PO relationship (Barstow and Molé 1991; Jones et al. 2011). Jones et al. (2011) state that the $\dot{V}O_{2sc}$ represents an increased cost of O_2 associated (decreased efficiency) with movement lasting greater than three minutes with PO above the GET and below the respiratory compensation point (RCP). While the mechanistic bases behind the $\dot{V}O_{2sc}$ have been debated for many years, there is a consensus that the $\dot{V}O_{2sc}$ during constant power exercise is related to the increased recruitment of type II muscle fibers (Jones et al. 2011).

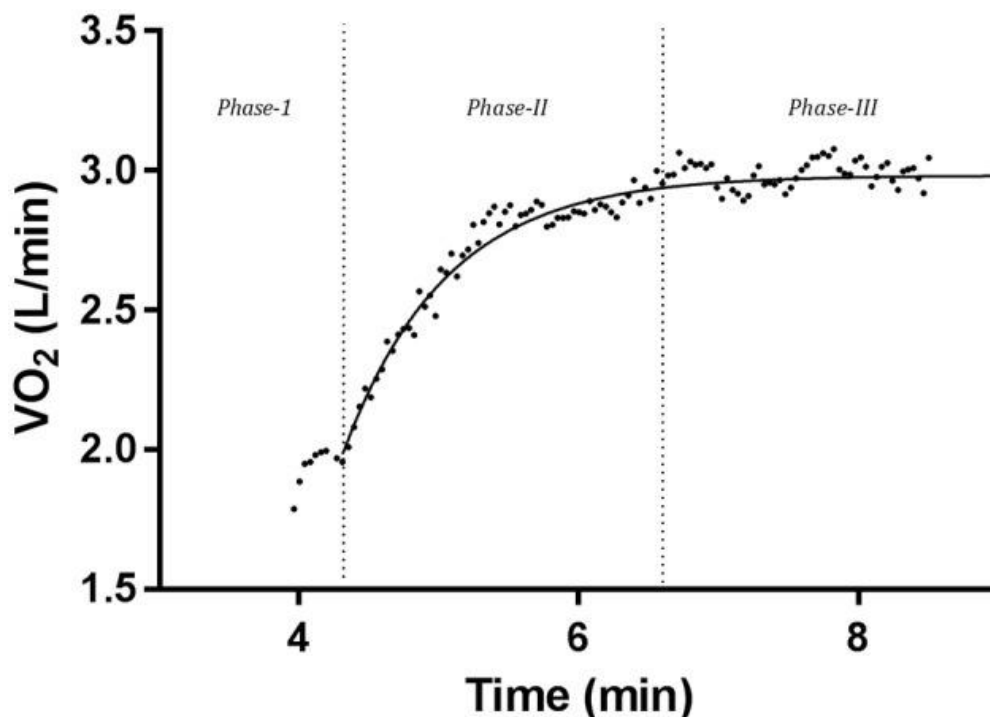


Figure 5. Example of an individual's oxygen uptake ($\dot{V}O_2$) kinetics data, organized into the three-phase approach. Phase I, also known as the cardiodynamic component, is a representation of the circulatory transit delay from muscles to the lungs. Phase II represents an exponential increase in $\dot{V}O_2$ due to increased blood flow both to the lungs and skeletal muscle, and subsequently deoxygenated venous blood returning to the lungs. Phase III reflects the achievement of a steady-state $\dot{V}O_2$ in the moderate-intensity domain, or a delayed achievement of a steady-state within the heavy-intensity domain (McNulty and Robergs 2017).

1.3 « Models for determining the MRT »

When modelling $\dot{V}O_2$ kinetics during constant power exercise, MRT refers to the time required to reach approximately 63% of the steady-state $\dot{V}O_2$ at a specific PO and is also the time constant of the exponential function used to describe this increase, denoted by the symbol τ within the literature (Whipp and Ward 1990; Sietsema et al. 1994). However, during RAMP, it represents a combined delay indicating two parameters: (1) the time interval representing $\dot{V}O_2$ muscle kinetics changes in response to increased ATP demand and (2) the transit delay of deoxygenated blood from muscles that are expressed at the lungs (Boone and Bourgois 2012a; Iannetta et al. 2019b). For the purposes of this study, MRT is in reference to the latter concept as applied to RAMP exercise.

During RAMP, the $\dot{V}O_2$ response to a linear increase in PO does not allow researchers to discern between the two aforementioned parameters of the MRT (Boone and Bourgois 2012a). Accounting for the MRT helps to accurately align $\dot{V}O_2$ with the PO and is a necessary instrument to avoid the designation of a greater $\dot{V}O_2$ than is present (Keir et al. 2018). There are two well-established models and one novel method to determine the MRT: the exponential model (MRT_{EXP}), the double-linear model (MRT_{LIN}), and the steady-state correction method (MRT_{SS}). It should be noted that the calculation of MRT values using nonlinear and linear models can be affected by the pre-ramp $\dot{V}O_2$ baseline, the amplitude of the $\dot{V}O_2$ change (gain; $\Delta\dot{V}O_2/\Delta PO$), the pre-ramp baseline power output, and training status (Boone et al. 2008; Iannetta et al. 2019b). At baseline there is approximately a 37% variability in $\dot{V}O_2$ within participants on any given day (Markovitz et al. 2004). This variable $\dot{V}O_2$ baseline will affect MRT calculations in both the non-linear and linear regression models. Furthermore, the slope of a RAMP affects the gain observed during the test as slower ramp protocols (i.e., 5, 10, 15 W/min) can artificially lengthen the MRT due to an increased gain (Hughson and Inman 1986; Iannetta et al. 2019a). Additionally, a lower baseline PO (≤ 20 W) can also lengthen the MRT value generated by these regression models as a result of inefficient energy transfer between the legs and bicycle crank ((Kautz et al.; Boone et al. 2008; Iannetta et al. 2019b). Moreover, a familiarity or training status effect has also been found to affect the MRT, as $\dot{V}O_2$ kinetics are shortened leading to a shorter MRT (Boone et al. 2008). These factors inherent to a RAMP test can cause poor reproducibility of the MRT values garnered by these models (Hughson and Inman 1986; Markovitz et al. 2004; Boone and Bourgois 2012a; Iannetta et al. 2019b). However, despite these inherent variables the model corrections provide a much better reflection of the actual PO $\dot{V}O_2$ relationship during RAMP.

1.3.1 Mono-Exponential correction method

This method is derived from the underlying concepts of $\dot{V}O_2$ kinetics during step-incremental exercise and the exponential nature of the $\dot{V}O_2$ response (phase II response). Introduced first by Whipp et al. (1981) this model incorporates a mono-exponential function to calculate the rate at which $\dot{V}O_2$ increases during phase II in a step-transition:

$$\dot{V}O_2(t) = \dot{V}O_{2BSL} + \Delta\dot{V}O_{2SS} \cdot [1 - e^{-(t-TD)/\tau}]$$

Where τ is the time required for $\dot{V}O_2$ to reach 63% the expected amplitude change at that power output ($\dot{V}O_{2SS}$) above baseline ($\dot{V}O_{2BSL}$), and TD is the time delay (Keir et al. 2018). Because a ramp-incremental exercise is the integral of a step-increment, this equation is then integrated to develop the following equation (Swanson and Hughson 1988; Keir et al. 2018):

$$\dot{V}O_2(t) = \dot{V}O_{2BSL} + \Delta\dot{V}O_{2SS} (t - \tau' \left[1 - e^{-\frac{1}{\tau'}} \right])$$

Where $\dot{V}O_2(t)$ is the value of $\dot{V}O_2$ at any time during the ramp, $\dot{V}O_{2BSL}$ is the pre-ramp baseline value (computed from the last 2 minutes before ramp onset), $\Delta\dot{V}O_{2SS}$ is the increment above $\dot{V}O_{2BSL}$ required for the power output at time t , and τ' is the effective time constant of the response.

1.3.2 Double-linear correction method

An alternative method used to account for $\dot{V}O_2$ kinetics during RAMP uses a double-linear model. In this model, the MRT is associated with the difference in time between the onset of the ramp exercise and the intersection of the backwards extrapolation of the $\dot{V}O_2$ vs time relationship MRT_{LIN} (figure 6) (Boone and Bourgois 2012a; Keir et al. 2018). The equation is as follows (taken from Keir et al. 2018):

$$f = \text{if } t < \text{MRT use } g(t), \text{ else } h(t); g(t) = i_1 + s_1t; i_2 = i_1 + s_1t; h(t) = i_2 + s_2t - \text{MRT}$$

where t is time, MRT is the time corresponding to the intersection of the two regression lines g and h are $\dot{V}O_2$, i_1 , s_1 and i_2 , s_2 are the intercepts and slopes of the first and second linear functions, respectively. s_1 is fixed at zero, giving the baseline $\dot{V}O_2$.

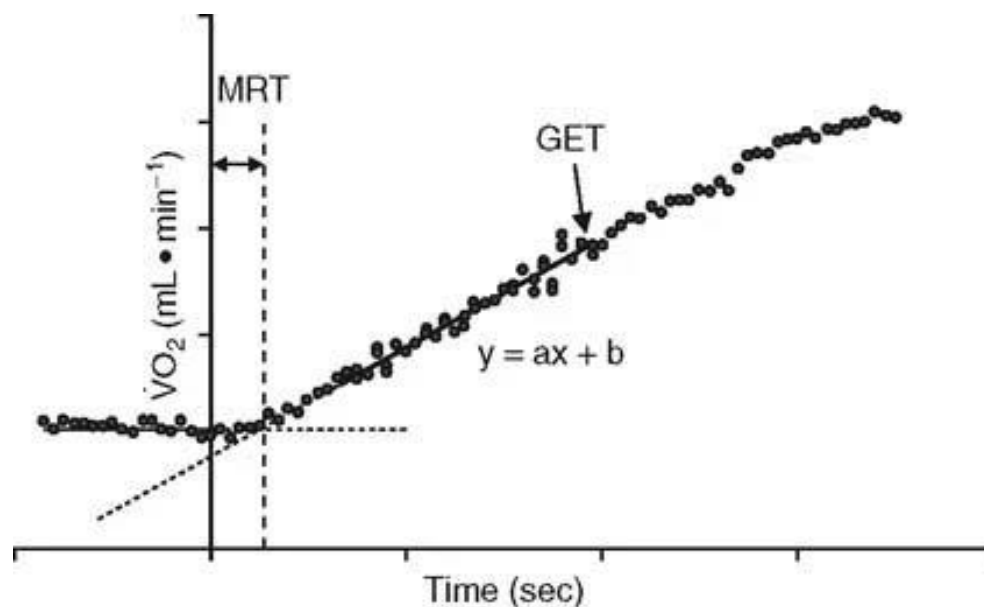


Figure 6. Example of the difference between ramp – incremental exercise (RAMP) onset (time = 0) and the intersection of the backwards extrapolation of the oxygen uptake ($\dot{V}O_2$) / time (t) relationship and extrapolation of the baseline $\dot{V}O_2$ to discern the time interval representing this individual's mean response time (MRT) (Boone and Bourgois 2012a).

1.3.3 Steady state correction method

As a result of reproducibility concerns associated with the regression models' calculations of MRT, Iannetta et al. (2019b) proposed a novel method (the steady-state method; MRT_{SS}) unencumbered by the factors that influence MRT calculation using linear or nonlinear regression modeling, resulting in greater reproducibility of the MRT. The procedure first requires a moderate-intensity step transition exercise test that is below the individual's GET, for a minimum of 6 minutes. The authors acknowledge that estimating an individual's GET can be challenging, and therefore suggest a 100W power rate, shown to be an adequate intensity for recreationally active and trained individuals (Iannetta et al. 2019b). However, for sedentary or older individuals, this value may be too high, and it is important to consider the population being tested. Nevertheless, once the step-transition test is done, a steady-state $\dot{V}O_2$ at a known power output is determined. Once the ramp-incremental exercise test is completed a linear regression is used to fit the $\dot{V}O_2$ vs PO relationship from the onset of rise in $\dot{V}O_2$ to the GET. Then, the steady-state $\dot{V}O_2$ previously determined from the moderate-step transition test is superimposed on this ramp $\dot{V}O_2$ /PO relationship. The difference between the (1) power output at the steady state $\dot{V}O_2$ from the step-

transition and (2) the power output at that same $\dot{V}O_2$ observed from the ramp-incremental exercise, is calculated in W (Figure 7). Depending on the ramp rate used, the watts are then converted into time (i.e., 1 W = 2s for a 30 W \cdot min $^{-1}$ ramp rate) (Iannetta et al. 2019b).

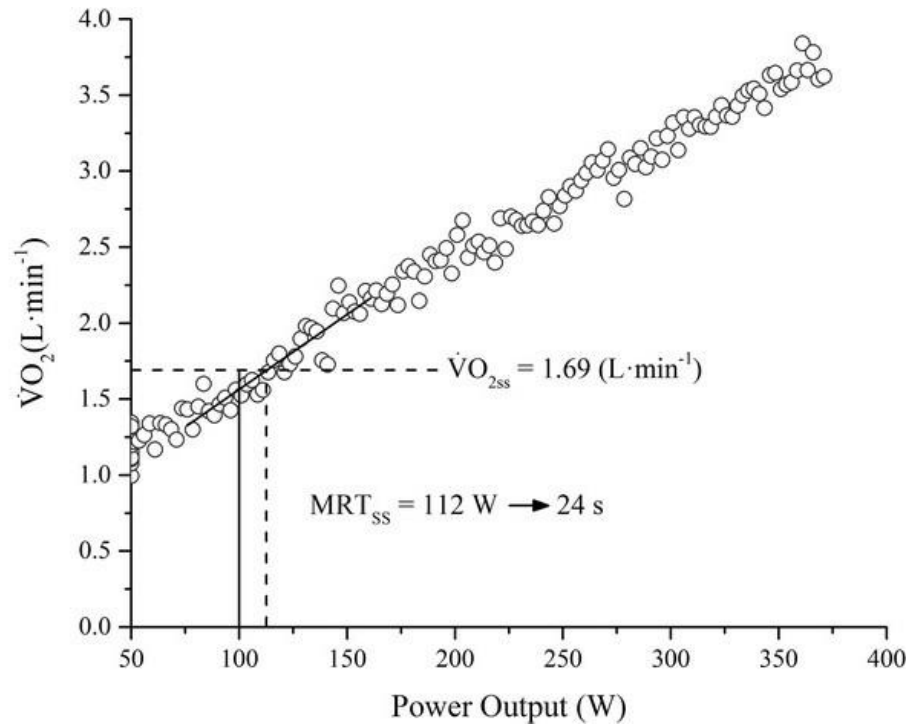


Figure 7. Example of the difference in power output (PO; measured in Watts, W) between the steady-state $\dot{V}O_2$ (100 W, solid line) and the power output associated with the ramp – incremental (RAMP) $\dot{V}O_2$ (112 W, dotted line). The difference was equivalent to 12 W, which, at a ramp rate of 30W \cdot min $^{-1}$ is 24 seconds (s) and is equivalent to the mean response time (MRT_{SS}) (Iannetta et al. 2019b).

1.4 « References »

- Arnold DL, Matthews PM, Radda GK (1984) Metabolic Recovery After Exercise and The Assessment of Mitochondrial Function In Vivo In Human Skeletal Muscle by Means of ^{31}P NMR. *Magnetic Resonance in Medicine* 1:307–315.
<https://doi.org/10.1002/Mrm.1910010303>
- B. Andrews Z (2010) Uncoupling Protein-2 And the Potential Link Between Metabolism and Longevity. *Current Aging Science* 3:102–112.
<https://doi.org/10.2174/1874609811003020102>
- Baird MF, Graham SM, Baker JS, Bickerstaff GF (2012) Creatine-Kinase- And Exercise-Related Muscle Damage Implications for Muscle Performance and Recovery. *Journal of Nutrition and Metabolism* 2012: <https://doi.org/10.1155/2012/960363>
- Barstow TJ, Lamarra N, Whipp BJ (1990) Modulation of Muscle and Pulmonary O_2 Uptakes by Circulatory Dynamics During Exercise. *Journal of Applied Physiology* (1985) 68:979–89. <https://doi.org/10.1152/Jappl.1990.68.3.979>
- Barstow TJ, Molé PA (1991) Linear and Nonlinear Characteristics of Oxygen Uptake Kinetics During Heavy Exercise. *Journal of Applied Physiology* (1985) 71:2099–2106.
<https://doi.org/10.1152/JAPPL.1991.71.6.2099>
- Bartee L, Shriner W, Creech C (2017) How Cells Obtain Energy. In *Principles of Biology*. Open Oregon Educational Resources.
- Beaver WL, Wasserman K, Whipp BJ (1985) Improved Detection of Lactate Threshold During Exercise Using a Log-Log Transformation. *Journal of Applied Physiology* 59:1936–1940. <https://doi.org/10.1152/Jappl.1985.59.6.1936>
- Bendahan D, Confort-Gouny S, Kozak-Reiss G, Cozzone PJ (1990) Heterogeneity of Metabolic Response to Muscular Exercise in Humans. New Criteria Of Invariance Defined By In Vivo Phosphorus-31 NMR Spectroscopy. *FEBS Letters*, 272(1-2), 155–158. [https://doi.org/10.1016/0014-5793\(90\)80472-U](https://doi.org/10.1016/0014-5793(90)80472-U)

- Bertuzzi R, Nascimento EM, Urso RP, Damasceno M, Lima-Silva AE (2013) Energy System Contributions During Incremental Exercise Test. *Journal of Sports Science & Medicine*, 12(3), 454–460.
- Bonora M, Patergnani S, Rimessi A, De Marchi E, Suski JM, Bononi A, Giorgi C, Marchi S, Missiroli S, Poletti F, Wieckowski MR, Pinton P (2012) ATP synthesis and storage. *Purinergic Signalling*, 8(3), 343–357. <https://doi.org/10.1007/s11302-012-9305-8>
- Boone J, Bourgois J (2012) The Oxygen Uptake Response to Incremental Ramp Exercise: Methodological and Physiological Issues. *Sports Medicine* 42:511–526. <https://doi.org/10.2165/11599690-000000000-00000>
- Boone J, Koppo K, Bouckaert J (2008) The $\dot{V}O_2$ Response to Submaximal Ramp Cycle Exercise: Influence of Ramp Slope and Training Status. *Respiratory Physiology & Neurobiology* 161:291–297. <https://doi.org/10.1016/j.resp.2008.03.008>
- Caen K, Bourgois JG, Stassijns E, Boone J (2022) A Longitudinal Study on The Interchangeable Use of Whole-Body and Local Exercise Thresholds In Cycling. *European Journal of Applied Physiology* 122:1657–1670. <https://doi.org/10.1007/S00421-022-04942-2>
- Cerezuela-Espejo V, Courel-Ibáñez J, Morán-Navarro R, Et Al (2018) The Relationship Between Lactate and Ventilatory Thresholds in Runners: Validity and Reliability Of Exercise Test Performance Parameters. *Frontiers in Physiology* 9: <https://doi.org/10.3389/fphys.2018.01320>
- Chaudhry R, Varacallo M (2022) Biochemistry, Glycolysis. In Statpearls. Statpearls Publishing.
- Colosio AL, Caen K, Bourgois JG, Boone J, Pogliaghi S (2020) Bioenergetics of The $\dot{V}O_2$ Slow Component Between Exercise Intensity Domains. *Plügers Archiv European Journal of Physiology* 472(10):1447–1456. <https://doi.org/10.1007/S00424-020-02437-7>

- Cooper GM (2000) *The Cell: A Molecular Approach*. ASM Press; Sinauer Associates, Washington, D.C.; Sunderland, Mass.
- Di Mauro S (2007) Muscle Glycogenoses: An Overview. *Acta Myologica* 26:35–41
- Gastin PB (2001) Energy System Interaction and Relative Contribution During Maximal Exercise. *Sports Medicine* 31:725–741. <https://doi.org/10.2165/00007256-200131100-00003/FIGURES/5>
- Glaister M (2005) Multiple Sprint Work Physiological Responses, Mechanisms of Fatigue and The Influence of Aerobic Fitness. *Sports Medicine*, 35(9), 757-777. <https://doi.org/10.2165/00007256-200535090-00003>
- Gløersen Ø, Colosio AL, Boone J, Dysthe DK, Malthe-Sørensen A, Capelli C, Pogliaghi S (2022) Modeling $\dot{V}O_2$ On-Kinetics Based on Intensity-Dependent Delayed Adjustment and Loss Of Efficiency (DALE). *Journal of Applied Physiology* 132:1480–1488. <https://doi.org/10.1152/Jappphysiol.00570.2021>
- Grassi B (2000) Skeletal Muscle $\dot{V}O_2$ On-Kinetics: Set by O_2 Delivery or by O_2 Utilization? New Insights into An Old Issue. *Medicine & Science in Sports & Exercise* 108. <https://doi.org/10.1097/00005768-200001000-00017>
- Grassi B (2005) Delayed Metabolic Activation of Oxidative Phosphorylation in Skeletal Muscle at Exercise Onset. *Medicine & Science in Sports & Exercise* 37:1567–1573. <https://doi.org/10.1249/01.Mss.0000177472.67419.0a>
- Guimarães-Ferreira L (2014) Role of The Phosphocreatine System on Energetic Homeostasis In Skeletal And Cardiac Muscles. *Einstein (Sao Paulo, Brazil)* 12:126-131. <https://doi.org/10.1590/S1679-45082014RB2741>
- Hughson RL, Inman MD (1986) Oxygen Uptake Kinetics from Ramp Work Tests: Variability Of Single Test Values. *Journal of Applied Physiology* 61:373–376. <https://doi.org/10.1152/Jappl.1986.61.1.373>

- Iannetta D, De Almeida Azevedo R, Keir DA, Murias JM (2019a) Establishing the $\dot{V}O_2$ Versus Constant-Work-Rate Relationship from Ramp-Incremental Exercise: Simple Strategies for An Unsolved Problem. *Journal Of Applied Physiology* 127:1519–1527. <https://doi.org/10.1152/jappphysiol.00508.2019>
- Iannetta D, Inglis EC, Pogliaghi S, Murias JM, Keir DA (2020b) A “Step-Ramp-Step” Protocol to Identify the Maximal Metabolic Steady State. *Medicine & Science in Sports & Exercise* 52:2011–2019. <https://doi.org/10.1249/MSS.0000000000002343>
- Iannetta D, Murias JM, Keir DA (2019b) A Simple Method to Quantify The V-O₂ Mean Response Time of Ramp-Incremental Exercise. *Medicine & Science in Sports & Exercise* 51:1080–1086. <https://doi.org/10.1249/MSS.0000000000001880>
- Iotti S, Lodi R, Frassinetti C, Zaniol P, Barbiroli B (1993) In Vivo Assessment of Mitochondrial Functionality in Human Gastrocnemius Muscle By³¹P MRS. The Role of pH in the Evaluation of Phosphocreatine and Inorganic Phosphate Recoveries from Exercise. *NMR in Biomedicine* 6:248–253. <https://doi.org/10.1002/Nbm.1940060404>
- Jin ES, Sherry AD, Malloy CR (2013) Metabolism of Glycerol, Glucose, And Lactate in The Citric Acid Cycle Prior To Incorporation into Hepatic Acylglycerols. *Journal of Biological Chemistry* 288:14488. <https://doi.org/10.1074/JBC.M113.461947>
- Jones AM, Grassi B, Christensen PM, Krstrup P, Bangsbo J, Poole DC (2011) Slow Component of $\dot{V}O_2$ Kinetics: Mechanistic Bases and Practical Applications. *Medicine & Science in Sports & Exercise* 43:2046–2062. <https://doi.org/10.1249/MSS.0B013E31821FCFC1>
- Jones AM, Poole DC (2005) Oxygen Uptake Dynamics: From Muscle to Mouth—An Introduction to The Symposium. *Medicine & Science in Sports & Exercise* 37:1542–1550. <https://doi.org/10.1249/01.Mss.0000177466.01232.7e>
- Jones AM, Wilkerson DP, Fulford J (2008) Muscle [Phosphocreatine] Dynamics Following the Onset Of Exercise In Humans: The Influence Of Baseline Work-Rate. *Journal of Physiology* 586:889. <https://doi.org/10.1113/JPHYSIOL.2007.142026>

- Kautz, S. A., & Neptune, R. R. (2002). Biomechanical Determinants of Pedaling Energetics: Internal and External Work Are Not Independent. *Exercise And Sport Sciences Reviews*, 30(4), 159–165. <https://doi.org/10.1097/00003677-200210000-00004>
- Keir DA, Iannetta D, Mattioni Maturana F, Kowalchuk JM, Murias JM (2022) Identification of Non-Invasive Exercise Thresholds: Methods, Strategies, and an Online App. *Sports Medicine* 52:237–255. <https://doi.org/10.1007/s40279-021-01581-z>
- Keir DA, Paterson DH, Kowalchuk JM, Murias JM (2018) Using Ramp-Incremental $\dot{V}O_2$ Responses for Constant-Intensity Exercise Selection. *Journal of Applied Physiology Nutrition and Metabolism*. 43(9): 882–892. <https://doi.org/10.1139/apnm-2017-0826>
- Kemp GJ, Taylor DJ, Radda GK (1993) Control of Phosphocreatine Resynthesis During Recovery from Exercise in Human Skeletal Muscle. *NMR in Biomedicine* 6:66–72. <https://doi.org/10.1002/nbm.1940060111>
- Korzeniewski B, Zoladz JA (2015) Possible Mechanisms Underlying Slow Component of $\dot{V}O_2$ On-Kinetics In Skeletal Muscle. *Journal of Applied Physiology* 118: 1240–1249. <https://doi.org/10.1152/jappphysiol.00027.2015>
- Macintosh BR, Murias JM, Keir DA, Weir JM (2021) What Is Moderate to Vigorous Exercise Intensity? *Frontiers in Physiology* 12:682233. <https://doi.org/10.3389/fphys.2021.682233>
- Mahler M (1985) First-Order Kinetics of Muscle Oxygen Consumption, and An Equivalent Proportionality Between $\dot{Q}O_2$ And Phosphorylcreatine Level. Implications For the Control of Respiration. *Journal of General Physiology* 86:135–165. <https://doi.org/10.1085/jgp.86.1.135>
- Markovitz GH, Sayre JW, Storer TW, Cooper CB (2004) On Issues of Confidence in Determining the Time Constant For Oxygen Uptake Kinetics. *British Journal of Sports Medicine* 38:553. <https://doi.org/10.1136/bjism.2003.004721>

- McMahon S, Jenkins D (2002) Factors Affecting the Rate of Phosphocreatine Resynthesis Following Intense Exercise. *Sports Medicine* 32:761–784.
<https://doi.org/10.2165/00007256-200232120-00002>
- McNulty CR, Robergs RA (2017) New Methods for Processing and Quantifying $\dot{V}O_2$ Kinetics To Steady State: $\dot{V}O_2$ Onset Kinetics. *Frontiers in Physiology* 8:740.
<https://doi.org/10.3389/fphys.2017.00740>
- Melkonian EA, Schury MP (2022) Biochemistry, Anaerobic Glycolysis. In StatPearls. StatPearls Publishing.
- Meyer RA (1988) A Linear Model of Muscle Respiration Explains Monoexponential Phosphocreatine Changes. *American Journal of Physiology-Cell Physiology* 254:C548–C553. <https://doi.org/10.1152/Ajpcell.1988.254.4.C548>
- Murias JM, Spencer MD, Kowalchuk JM, Paterson DH (2011) Influence of Phase I Duration on Phase II $\dot{V}O_2$ Kinetics Parameter Estimates In Older And Young Adults. *American Journal of Physiology-Regulatory, Integrative and Comparative Physiology* 301: R218–R224. <https://doi.org/10.1152/Ajpregu.00060.2011>
- Murias JM, Spencer MD, Paterson DH (2014) The Critical Role of O_2 Provision in The Dynamic Adjustment Of Oxidative Phosphorylation. *Exercise and Sport Sciences Reviews* 42:4–11. <https://doi.org/10.1249/JES.0000000000000005>
- Muscella A, Stefàno E, Lunetti P, Capobianco L, Marsigliante S (2020) The Regulation of Fat Metabolism During Aerobic Exercise. *Biomolecules* 10:1–29.
<https://doi.org/10.3390/BIOM10121699>
- Nolfi-Donagan D, Braganza A, Shiva S (2020) Mitochondrial Electron Transport Chain: Oxidative Phosphorylation, Oxidant Production, And Methods of Measurement. *Redox Biology* 37:101674. <https://doi.org/10.1016/J.Redox.2020.101674>
- Özyener F, Rossiter HB, Ward SA, Whipp BJ (2001) Influence of Exercise Intensity on The On-and Off-Transient Kinetics of Pulmonary Oxygen Uptake In Humans. *Journal of*

- Physiology 533:891–902. <https://doi.org/10.1111/J.1469-7793.2001.T01-1-00891.X>
- Pallarés JG, Morán-Navarro R, Ortega JF, Fernández-Elías VE, Mora-Rodríguez R (2016) Validity and Reliability Of Ventilatory and Blood Lactate Thresholds In Well-Trained Cyclists. *Plos One* 11: E0163389. <https://doi.org/10.1371/Journal.Pone.0163389>
- Poole DC, Ward SA, Gardner GW, Whipp BJ (1988) Metabolic and Respiratory Profile of The Upper Limit For Prolonged Exercise In Man. *Ergonomics* 31:1265–1279. <https://doi.org/10.1080/00140138808966766>
- Purdom T, Kravitz L, Dokladny K, Mermier C (2018) Understanding the Factors That Effect Maximal Fat Oxidation. *Journal of the International Society of Sports Nutrition* 15 (1):3. <https://doi.org/10.1186/S12970-018-0207-1>
- Sietsema KE, Ben-Dov I, Zhang YY, Sullivan C, Wasserman K (1994) Dynamics of Oxygen Uptake for Submaximal Exercise And Recovery In Patients With Chronic Heart Failure. *Chest Journal* 105:1693–1700. <https://doi.org/10.1378/CHEST.105.6.1693>
- Swanson GD, Hughson RL (1988) On the Modeling and Interpretation of Oxygen Uptake Kinetics from Ramp Work Rate Tests. *Journal Of Applied Physiology* 65(6), 2453–2458. <https://doi.org/10.1152/Jappl.1988.65.6.2453>
- Thompson CH, Kemp GJ, Sanderson AL, Radda GK (1995) Skeletal Muscle Mitochondrial Function Studied by Kinetic Analysis of Postexercise Phosphocreatine Resynthesis. *Journal of Applied Physiology* 78:2131–2139. <https://doi.org/10.1152/Jappl.1995.78.6.2131>
- Wasserman K, Beaver WL, Whipp BJ (1986) Mechanisms and Patterns of Blood Lactate Increase During Exercise In Man. *Medicine & Science in Sports & Exercise* 18:344–352. <https://doi.org/10.1249/00005768-198606000-00017>

- Wasserman K, Whipp BJ, Koysl SN, Beaver WL (1973) Anaerobic Threshold and Respiratory Gas Exchange During Exercise. *Journal of Applied Physiology* 35:236–243. <https://doi.org/10.1152/Jappl.1973.35.2.236>
- Whipp BJ, Davis JA, Torres F, Wasserman K (1981) A Test to Determine Parameters of Aerobic Function During Exercise. *Journal Of Applied Physiology* 50:217–221. <https://doi.org/10.1152/Jappl.1981.50.1.217>
- Whipp BJ, Ward SA (1990) Physiological Determinants of Pulmonary Gas Exchange Kinetics During Exercise. *Medicine & Science in Sports & Exercise* 22:62–71
- Whipp, B. J., Ward, S. A., Lamarra, N., Davis, J. A., & Wasserman, K. (1982). Parameters Of Ventilatory and Gas Exchange Dynamics During Exercise. *Journal Of Applied Physiology: Respiratory, Environmental and Exercise Physiology*, 52(6), 1506–1513. <https://doi.org/10.1152/jappl.1982.52.6.1506>
- Xiao W, Wang RS, Handy DE, Loscalzo J (2018) NAD(H) And NADP(H) Redox Couples and Cellular Energy Metabolism. *Antioxidants & Redox Signaling* 28:251. <https://doi.org/10.1089/ARS.2017.7216>

Chapter 2

2 « A Comparison of Methods to Identify the Mean Response Time of Ramp-Incremental Exercise for Exercise Prescription »

2.1 « Introduction »

The oxygen uptake ($\dot{V}O_2$) versus power output (PO) relationship from ramp-incremental exercise (RAMP) is often used to prescribe aerobic exercise intensity (Pescatello 2014, Keir et al. 2018). During ramp-incremental exercise, as power output increases, there is a delay in the increase in the breath-by-breath $\dot{V}O_2$ that largely reflects the transit delay in muscle $\dot{V}O_2$ being reflected in $\dot{V}O_2$ response measured at the level of the mouth, and that contributes to a misalignment of $\dot{V}O_2$ to power output; this delay is known as the mean response time (MRT). If the MRT is not accounted for during the exercise prescription process, exercise at any ramp-identified power output will elicit a steady-state $\dot{V}O_2$ value that is higher than predicted. Thus, estimating and correcting for the MRT by “left shifting” power output relative to $\dot{V}O_2$ during ramp-incremental exercise is necessary to appropriately determine the steady-state $\dot{V}O_2$ for any constant power output below the lactate threshold (θ_{LT}) and within the moderate-intensity domain where $\dot{V}O_2$ kinetics remain constant (Spencer et al. 2013; Keir et al. 2015). However, at intensities above the lactate threshold, accounting for the MRT is insufficient as a correction method, due to the presence of the $\dot{V}O_2$ slow component ($\dot{V}O_{2sc}$) (Caen et al. 2020).

The MRT reflects the sum of the time it takes for deoxygenated blood from the active muscles to reach the lungs (transit delay) plus the time required for $\dot{V}O_2$ to achieve a value commensurate with the metabolic demand ($\dot{V}O_2$ kinetics). These two temporal components can vary widely from person to person and thus, to ensure accurate exercise prescription from ramp incremental testing (at least within the moderate intensity domain), MRT quantification should be made on an individual basis. Currently, there are three methods by which the MRT may be determined. The “exponential method” (MRT_{EXP}) utilizes a mono-exponential fit of the $\dot{V}O_2$ versus time

relationship (Swanson and Hughson, 1988) to derive an effective time constant (τ'). The “double-linear method” (MRT_{LIN}) applies a piecewise function to both the pre-transition baseline (with a fixed “zero” slope) and ramp-incremental data (with a variable slope) to derive a breakpoint that gives the MRT (Boone and Bourgois 2012). The “steady-state method” (MRT_{SS}) does not rely on fitting. Rather, a moderate-intensity step-transition (MOD) precedes the ramp-incremental protocol. The steady-state $\dot{V}O_2$ at this power output is then superimposed on the $\dot{V}O_2$ vs power output relationship from the ramp test and the difference in power output between MOD and the ramp-identified power output corresponding to the steady state $\dot{V}O_2$ of the MOD is computed to derive the MRT. Each of the three methods have demonstrated good-to-excellent reproducibility and, on average, MRT values computed using these different methods are not different (Iannetta et al. 2019b). However, yet to be examined, is a comparison amongst MRT methods with respect to their accuracy of predicting steady-state $\dot{V}O_2$ at a given power output below the lactate threshold.

With exercise above the lactate threshold, a $\dot{V}O_2$ slow component emerges that progressively delays the attainment of steady state $\dot{V}O_2$ and amplifies the $\dot{V}O_2$ gain ($\Delta\dot{V}O_2/PO$) (Whipp et al. 1982). In most ramp-incremental protocols, however, the non-linearity in the $\dot{V}O_2$ versus power output relationship is not observed because the progressively rising time constant and gain parameters associated with the action of the $\dot{V}O_2$ slow component balance to maintain linearity (Wilcox et al. 2016; Keir et al. 2016). Additionally, the $\dot{V}O_2$ slow component is not considered in the MRT concept. As a result, the MRT becomes insufficient to predict the steady-state $\dot{V}O_2$ for all power outputs above the lactate threshold and within the heavy-intensity domain (Barstow et al. 1993, Keir et al. 2018). Although some strategies have recently been developed to account for this nonlinearity in the $\dot{V}O_2$ versus power output relationship (Caen et al. 2020, Iannetta et al. 2019a), whether any of the three models used to estimate the MRT can be applied to predict steady-state $\dot{V}O_2$ responses within the lower regions of the heavy-intensity domain remains unclear.

The novel purpose of this study was to compare the three methods of MRT estimation and evaluate their accuracy at predicting $\dot{V}O_2$ at power outputs well below, slightly below and slightly above the lactate threshold. It was hypothesized that: i) MRT_{EXP} , MRT_{LIN} and MRT_{SS} would not be different from each other; ii) the prediction accuracies (defined as the difference between the $\dot{V}O_2$ predicted by a model-corrected ramp incremental to the $\dot{V}O_2$ measured during constant power

exercise at each intensity) between the MRT_{EXP} , MRT_{LIN} and MRT_{SS} models would not be different from one another; and iii) above the lactate threshold, all three models will underestimate the $\dot{V}O_2$ when compared to the steady state $\dot{V}O_2$ at that power output.

2.2 « Methods »

2.2.1.1 Participants

Upon providing written informed consent, ten recreationally active or highly trained (McKay et al. 2022) males (mean \pm SD, age = 25 ± 7 yr) participated in this study (Table 1). All volunteers were lifelong nonsmokers and were free of any respiratory, cardiovascular, musculoskeletal, and metabolic conditions that may impact cardiorespiratory or metabolic responses to exercise. The age of participants was not deemed a limiting factor as $\dot{V}O_2$ kinetics are unchanged across the age continuum of young, middle-aged or older individuals (Grey et al 2015). Each participant reported to the laboratory on 4 occasions to perform the following protocols at the Canadian Centre for Activity and Aging in the Health Science building on Western's campus. They were also instructed to refrain from physical activity on the day of testing, as well as to refrain from eating or ingesting caffeine for a period of two and eight hours respectively, before their testing appointment. This study was approved by the Western University Research Ethics Board for Health Sciences Research Involving Human Participants (see Appendix).

2.2.1.2 Equipment and Measurements

All trials were performed on an electromagnetically-braked cycle ergometer (Velotron, RacerMate, Seattle, WA). During all tests, heart rate was monitored (Cosmed heart rate band) and gas exchange and ventilatory variables were measured breath-by-breath by a metabolic cart (CPET; Cosmed, Rome, Italy). The apparatus consisted of a facemask and a low-dead-space turbine which was calibrated using a 3L syringe. Respired air was collected through a sampling line and fractional concentrations of inspired and expired O_2 and CO_2 for each breath were determined by gas analyzers that were calibrated prior to each test using a gas mixture of known concentration (16% O_2 , 5% CO_2 , balance N_2).

2.2.1.3 Experimental Protocol

During four visits separated by at least 48 h, participants performed a ramp-incremental exercise test and three constant-power exercise tests. In their initial visit, participants selected their own cadence (between 70–90 rpm) and were instructed to maintain this cadence throughout both ramp and constant-power protocols.

2.2.1.4 Ramp-incremental protocol

The protocol included a 4-min baseline at 20 W followed by a $30 \text{ W} \cdot \text{min}^{-1}$ ramp until task failure. The protocol was terminated once participants could not maintain their self-selected cadence for greater than 10 s despite strong verbal encouragement.

2.2.1.5 Constant power protocol

Each constant-power test began with 4-min of baseline cycling at 20 W, followed by a 30 min exercise bout at a set power output. Of the three tests, two were performed in the moderate intensity (75% and 85% of lactate threshold) domain and one in the heavy intensity domain (15% of the difference between lactate threshold and $\dot{V}O_{2\text{max}}$; $\Delta 15$). To ensure domain-specific responses, the power output associated with these bouts were determined by first identifying the $\dot{V}O_2$ values at 75%, 85%, and $\Delta 15$, respectively. Then, the $\dot{V}O_2$ vs time relationship was “left-shifted” by $2/3$ the ramp rate retrospectively (i.e., $30 \text{ W} \cdot \text{min}^{-1} = 20 \text{ W} = 40 \text{ s}$), an arbitrary method of MRT correction (Bailey et al. 2010; Whipp et al. 1981). The power outputs associated with this $\dot{V}O_2$ were located on the “corrected” $\dot{V}O_2$ vs power output relationship and used as the constant-power output. The steady-state $\dot{V}O_2$ associated with each constant-power test was computed as the average of the last 5 min. Capillary lactates were taken at rest and at the end of each 30-min trial. Capillary blood samples were drawn from a fingerprick and immediately analyzed for blood lactate concentration ($[\text{La}^-]_b$) to ensure that participants achieved the appropriate intensity.

2.2.2 Data Analysis

The data from the ramp-incremental test was used to determine participants’ maximal aerobic capacity ($\dot{V}O_{2\text{max}}$), and to estimate lactate threshold (θ_{LT}) and their associated power outputs. The

$\dot{V}O_{2\max}$ and θ_{LT} were determined using ExerciseThresholds.com—an online resource for the evaluation of gas exchange and ventilatory data (Keir et al. 2022). The $\dot{V}O_{2\max}$ was determined as the highest value from a 20-s rolling average. To determine θ_{LT} , profiles of ventilation (\dot{V}_E), gas exchange ($\dot{V}O_2$ and $\dot{V}CO_2$), and their combination ($\dot{V}_E/\dot{V}CO_2$, $\dot{V}_E/\dot{V}O_2$), as well as respiratory exchange ratio (RER), end-tidal partial pressure of O_2 and CO_2 were all plotted against $\dot{V}O_2$ and evaluated by two members of the investigative team until a consensus of θ_{LT} was reached. The $\dot{V}O_2$ vs time relationship was time aligned such that the onset of the ramp began at $t=0$. From these data, the MRT was estimated using the following three approaches:

Mono-exponential MRT (MRT_{EXP}). A mono-exponential function was fitted to the $\dot{V}O_2$ data from the onset of the ramp at $t = 0$ to the identified θ_{LT} . This function generates a τ' (hereafter referred to as “ MRT_{EXP} ,” Figure 8A).

$$4) \dot{V}O_2(t) = \dot{V}O_{2BSL} + \Delta\dot{V}O_{2SS} \left(t - \tau' \left[1 - e^{-\frac{t}{\tau'}} \right] \right)$$

where $\dot{V}O_2(t)$ is the value of $\dot{V}O_2$ at any time during the ramp, $\dot{V}O_{2BSL}$ is the pre-ramp baseline value (computed from the last 2 minutes before ramp onset), $\Delta\dot{V}O_{2SS}$ is the increment above $\dot{V}O_{2BSL}$ required for the power output at time t , and τ' is the effective time constant of the response.

Double-linear MRT (MRT_{LIN}). A piecewise function was applied to both the pre-ramp incremental baseline (with a fixed “zero” slope) and ramp-incremental data (with a variable slope) to derive a “breakpoint” that reflects the MRT_{LIN} (Boone and Bourgois 2012) (Figure 8B).

$$5) f = \begin{cases} g(t) & \text{if } t < MRT \\ h(t) & \text{else} \end{cases}; g(t) = i_1 + s_1t; i_2 = i_1 + s_1MRT; h(t) = i_2 + s_2t - MRT$$

where t is time, MRT is the time corresponding to the intersection of the two regression lines g and h are $\dot{V}O_2$, i_1 , s_1 and i_2 , s_2 are the intercepts and slopes of the first and second linear functions, respectively. s_1 was fixed at 0. i_1 was fitted from the last 2 min of the pre-ramp baseline to the time at which the $\dot{V}O_2$ associated with θ_{LT} was reached.

Steady-state MRT (MRT_{SS}). The steady-state $\dot{V}O_2$ from the 75% θ_{LT} condition was computed from all breaths within the last 5 minutes of exercise. Next, linear regression was applied to the ramp incremental $\dot{V}O_2$ versus power output relationship, including data from the first observable rise in

$\dot{V}O_2$ to $\dot{V}O_{2peak}$. Thereafter, the predicted ramp power output corresponding to steady-state $\dot{V}O_2$ from the 75% θ_{LT} trial was determined using the equation of the regression line. Lastly, the difference in power output at this $\dot{V}O_2$ from the ramp and the power output at 75% θ_{LT} was determined to calculate MRT_{SS} :

$$MRT_{SS} (W) = ([\dot{V}O_2 \text{ at } 75\% \theta_{LT} - \text{intercept}] / \text{slope}) - PO \text{ at } 75\% \theta_{LT} \quad (3)$$

where the intercept ($L \cdot \text{min}^{-1}$) and the slope ($L \cdot \text{min}^{-1} \cdot W^{-1}$) are obtained from the linear regression of the ramp $\dot{V}O_2$ response. This value was then converted to time (i.e., 1 W = 2 s for a 30 $W \cdot \text{min}^{-1}$ ramp) to give the MRT_{SS} in seconds (Figure 8C).

The MRT_{EXP} , MRT_{LIN} , and MRT_{SS} models were used to shift the $\dot{V}O_2$ vs time relationship at each intensity (75%, 85% and $\Delta 15 \theta_{LT}$) to predict the $\dot{V}O_2$ expected at each of the predetermined constant-power outputs ($\dot{V}O_2$ “predicted”). The accuracy of each model was evaluated by comparing the “predicted” $\dot{V}O_2$ to the “measured” $\dot{V}O_2$ at each intensity. “Predicted” $\dot{V}O_2$ at each power output was also determined without correction for the MRT (NO_{MRT}).

2.2.3 Statistical Analysis

Data were presented as means \pm SD. Two-Way repeated measures analysis of variance (ANOVA) was used to compare 1) the measured $\dot{V}O_2$ to each model-predicted- $\dot{V}O_2$ at 2) each of the three intensities (75%, 85%, $\Delta 15$). Statistical significance was accepted at an alpha level of 5%. All statistical analyses were performed using SigmaPlot Version 14.0 (Systat Software Inc., San Jose, CA). Power calculation: at 85% GET = 0.93; based on Minimum Detectable Difference in Means (217 ml), Expected Standard Deviation of Residuals (115), Number of Groups (4), and a Group Size (10), at an Alpha of 0.05. Sample size calculation at 85% GET was 9; Minimum Detectable Difference in Means (217 ml), Expected Standard Deviation of Residuals (115), Number of Groups (4), Desired Power (0.8), Alpha size (0.05).

2.3 « Results »

The group mean $\dot{V}O_{2max}$ was $3.69 \pm 0.72 L \cdot \text{min}^{-1}$; peak power output was $352 \pm 57 W$, and the $\dot{V}O_2$ at θ_{LT} was $2.22 \pm 0.69 L \cdot \text{min}^{-1}$. Applying a standard or fixed MRT correction factor equivalent to

2/3 the ramp rate (i.e., $30 \text{ W}\cdot\text{min}^{-1} = 20 \text{ W} = 40 \text{ s}$), these “left-shifted” power output values anticipated to elicit steady-state $\dot{V}O_2$ associated with $\sim 75\% \theta_{LT}$, $\sim 85\% \theta_{LT}$, and $\sim \Delta 15$, were $116 \pm 52 \text{ W}$, $140 \pm 65 \text{ W}$, and $181 \pm 64 \text{ W}$, respectively. During constant-power exercise at these intensities, the steady-state $\dot{V}O_2$ values were $1.83 \pm 0.55 \text{ L}\cdot\text{min}^{-1}$ ($82 \pm 6\% \theta_{LT}$), $2.09 \pm 0.73 \text{ L}\cdot\text{min}^{-1}$ ($93 \pm 8\% \theta_{LT}$), and $2.62 \pm 0.86 \text{ L}\cdot\text{min}^{-1}$ ($\Delta 27 \pm 23\% \theta_{LT}$).

The MRT values for MRT_{EXP} , MRT_{LIN} and MRT_{SS} were 45 s, 33 s, and 42 s, respectively (Figure 8) which corresponded to power outputs of 23 W, 17 W, and 21 W (Table 2). Compared to MRT_{SS} , MRT_{EXP} ($P = 0.372$) and MRT_{LIN} ($P = 0.372$) were not different. However, there was a difference between MRT_{EXP} and MRT_{LIN} ($P < 0.05$). The MRT-adjusted (i.e., MRT_{EXP} , MRT_{LIN} and MRT_{SS}) and MRT-unadjusted (i.e., NO_{MRT}) prediction of the steady-state $\dot{V}O_2$ for each constant-power output ride are presented in Table 3.

At $75\% \theta_{LT}$ the average steady-state $\dot{V}O_2$ measured during the constant-power output bout was $1.83 \pm 0.55 \text{ L}\cdot\text{min}^{-1}$. With MRT-adjustment by MRT_{EXP} , there was no difference ($P = 1.000$) between the MRT_{EXP} -predicted $\dot{V}O_2$ and the measured steady-state $\dot{V}O_2$ (mean bias: $31 \pm 98 \text{ mL}\cdot\text{min}^{-1}$). Similarly, the predicted $\dot{V}O_2$ from the MRT_{LIN} - and MRT_{SS} - corrected values also were not different ($P = 1.000$ for both; MRT_{LIN} mean bias: $-35 \pm 60 \text{ mL}\cdot\text{min}^{-1}$; MRT_{SS} -mean bias: $11 \pm 39 \text{ mL}\cdot\text{min}^{-1}$). Without MRT-adjustment (i.e., NO_{MRT}), this value was underestimated ($P < 0.05$), on average, by $167 \pm 111 \text{ mL}\cdot\text{min}^{-1}$ (Table 3 and Figure 9).

At $85\% \theta_{LT}$ the average steady-state $\dot{V}O_2$ measured during the constant-power output bout was $2.09 \pm 0.73 \text{ L}\cdot\text{min}^{-1}$. Compared to this measured $\dot{V}O_2$ value, there was no difference from $\dot{V}O_2$ values predicted by the MRT_{EXP} (mean bias: $-14 \pm 134 \text{ mL}\cdot\text{min}^{-1}$, $P = 1.00$), MRT_{LIN} (mean bias: $-79 \pm 112 \text{ mL}\cdot\text{min}^{-1}$, $P = 1.00$) and MRT_{SS} (mean bias: $-32 \pm 91 \text{ mL}\cdot\text{min}^{-1}$, $P = 1.00$) (Figure 9). NO_{MRT} consistently predicted a $\dot{V}O_2$ value that was lower than the measured $\dot{V}O_2$ at $85\% \theta_{LT}$ by an average of $217 \pm 115 \text{ mL}\cdot\text{min}^{-1}$.

The average steady-state $\dot{V}O_2$ measured during the constant-power output bout at $\Delta 15$ was $2.62 \pm 0.89 \text{ L}\cdot\text{min}^{-1}$. NO_{MRT} consistently predicted a $\dot{V}O_2$ value that was lower than that measured at $\Delta 15$ (mean bias: $-392 \pm 345 \text{ mL}\cdot\text{min}^{-1}$). There was no difference ($P = 0.767$) between MRT_{EXP} -predicted $\dot{V}O_2$ and the measured steady-state $\dot{V}O_2$ at $\Delta 15$ (mean bias: $98 \pm 433 \text{ mL}\cdot\text{min}^{-1}$). However, the

MRT_{LIN} and MRT_{SS} predicted $\dot{V}O_2$ values were lower ($P < 0.05$) than the measured $\dot{V}O_2$ (mean bias: $-254 \pm 323 \text{ mL}\cdot\text{min}^{-1}$; $-206 \pm 300 \text{ mL}\cdot\text{min}^{-1}$, respectively; Figure 9).

Table 1. Participant characteristics and results from the ramp incremental test (n=10).

Participant	Age	$\dot{V}O_{2max}$	PO at $\dot{V}O_{2max}$ (W)	θ_{LT} ($\dot{V}O_2$ L*min ⁻¹)	θ_{LT} (W)
1	26	3.11	300	1.60	135
2	24	2.92	303	1.77	150
3	22	3.91	376	1.68	130
4	21	3.26	303	2.25	195
5	46	3.08	300	1.50	110
6	21	5.13	449	3.40	265
7	21	4.32	413	3.00	252
8	21	4.35	416	3.05	250
9	21	3.31	336	2.15	180
10	23	3.47	325	1.81	140
Mean	25	3.69	352	2.22	181
SD	8	0.72	57	0.69	57

$\dot{V}O_{2max}$, maximum oxygen uptake; PO, power output; W, watts; θ_{LT} , estimated lactate threshold; SD, standard deviation.

Table 2. Mean response time of the three methods expressed in seconds(s) and Watts (W)

Participant	MRT _{EXP} (s)	MRT _{LIN} (s)	MRT _{SS} (s)	MRT _{EXP} (W)	MRT _{LIN} (W)	MRT _{SS} (W)
1	67	49	46	33	24	23
2	18	14	40	9	7	20
3	90	55	54	45	28	27
4	76	59	62	38	29	31
5	40	19	38	20	9	19
6	13	11	6	6	6	3
7	39	28	10	19	14	5
8	41	37	48	21	18	24
9	53	48	72	27	24	36
10	15	14	44	7	7	22
Mean	45	33*	42	23	17*	21
SD	26	18	21	13	9	10

S, seconds; MRT_{EXP}, the time delay associated with the exponential model; MRT_{LIN}, the time delay associated with the double-linear model; MRT_{SS} the time delay associated with the steady-state method; * indicates a significant difference from MRT_{EXP}.

Table 3. Mean, SD, and Range of the bias from each predictive method at different intensities

Intensity (% of θ_{LT})	NO_{MRT} pred.				
	minus measured $\dot{V}O_2(\text{mL}\cdot\text{min}^{-1})$ 1)	MRT_{EXP} pred. minus measured $\dot{V}O_2(\text{mL}\cdot\text{min}^{-1})$	MRT_{LIN} pred. minus measured $\dot{V}O_2(\text{mL}\cdot\text{min}^{-1})$	MRT_{SS} pred. minus measured $\dot{V}O_2(\text{mL}\cdot\text{min}^{-1})$	
75%	Mean	-167* [†] ^β	31	-35	11
	SD	111	98	60	34
	Min – Max	-346 — 15	-99 — 197	-120 — 57	-39 — 46
85%	Mean	-217* [†] ^β	-14 [†]	-79	-32
	SD	115	134	112	91
	Min – Max	-411 — -102	-208 — 194	-227 — 99	-177 — 83
Δ15	Mean	-392* [†] ^β	-98	-254*	-206*
	SD	245	433	323	301
	Min – Max	-942 — -60	-890 — 720	-1005 — 115	-914 — 168

MRT_{EXP} pred., the predicted $\dot{V}O_2$ using the exponential model; MRT_{LIN} pred. $\dot{V}O_2$, predicted $\dot{V}O_2$ using the double-linear model; MRT_{SS} pred., predicted $\dot{V}O_2$ using the steady-state model; NO_{MRT} pred. $\dot{V}O_2$, ramp-associated $\dot{V}O_2$ with no correction model applied; measured $\dot{V}O_2$, $\dot{V}O_2$ observed from the last 5 min of the 30 min constant load θ_{LT} trial at a specific intensity; Δ15, 15% of the difference between θ_{LT} and $\dot{V}O_{2\text{max}}$; SD, standard deviation

* Significantly different from measured $\dot{V}O_2$ at the respective intensity

[†] Significantly different from MRT_{EXP} pred. minus measured $\dot{V}O_2$

^β Significantly different from MRT_{SS} pred. minus measured $\dot{V}O_2$

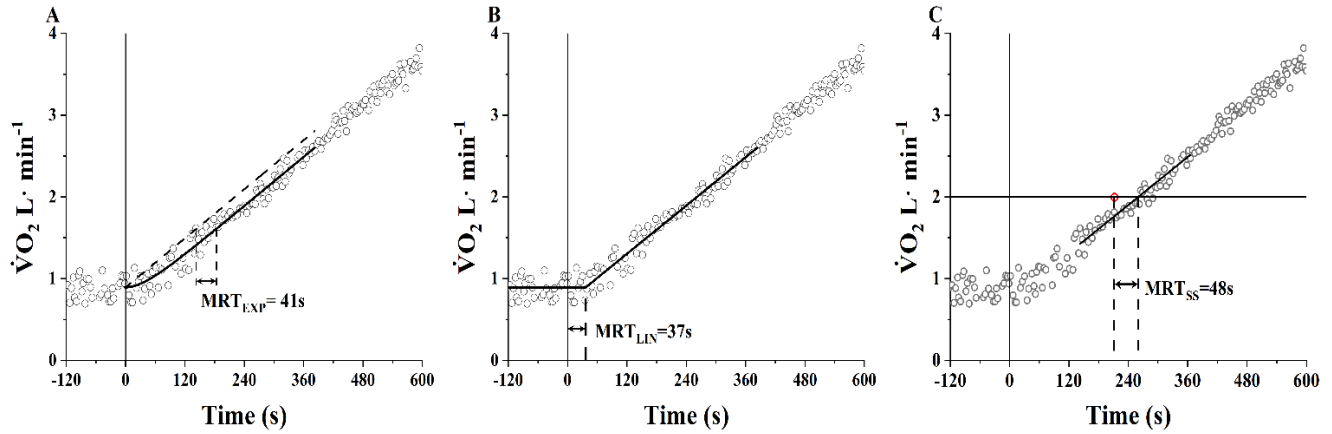


Figure 8. Mean Response Time (MRT) values at 75% estimated lactate threshold (θ_{LT}) of a representative individual of the mean response time for an exponential model (A, MRT_{EXP}), the double-linear model (B, MRT_{LIN}), and steady-state method (C, MRT_{SS} ; determined using linear interpolation of $\dot{V}O_2$ determined from the three constant load protocols).

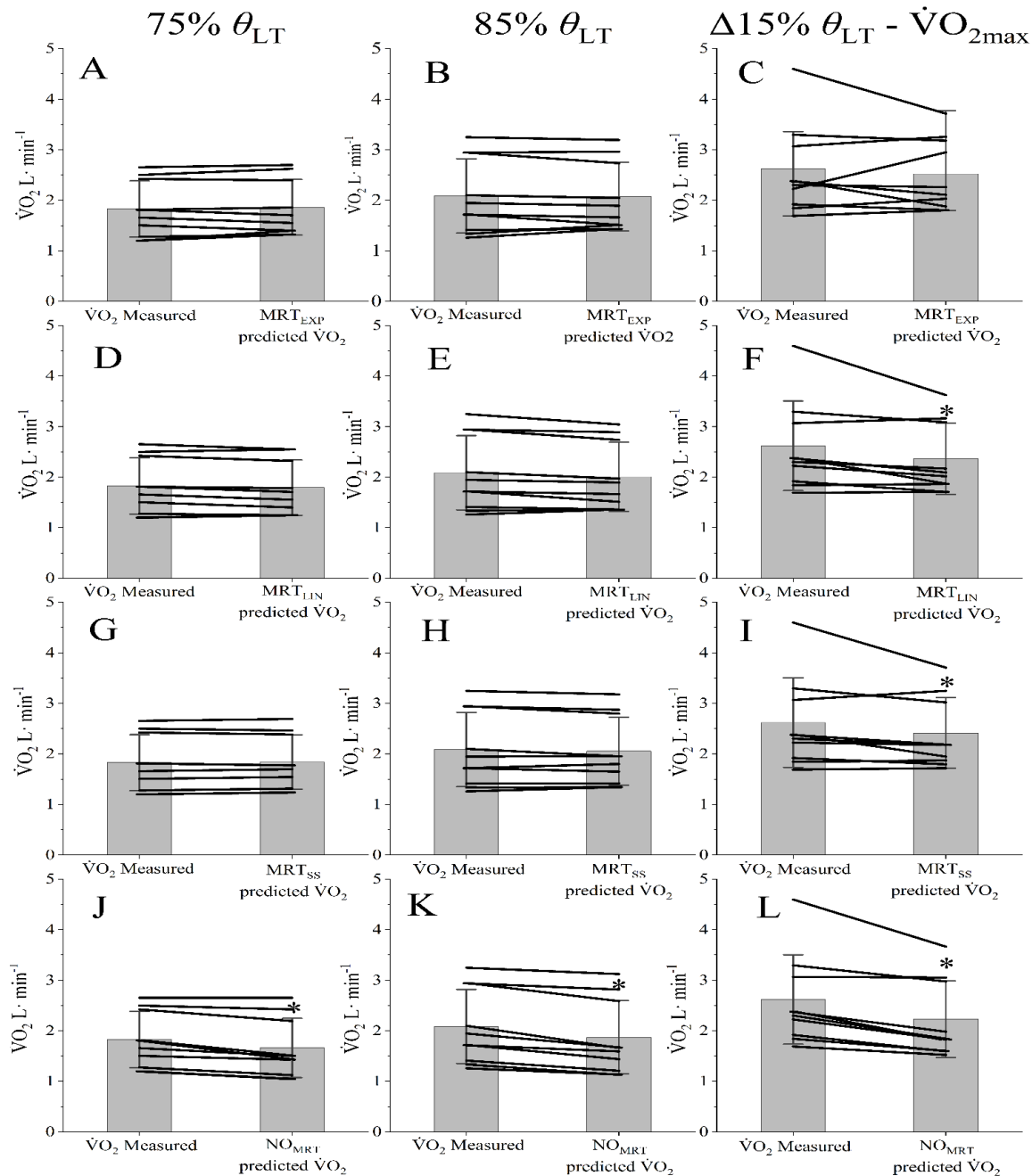


Figure 9. Bar graphs showing mean \pm SD. Lines connect individual measured $\dot{V}O_2$ with predicted $\dot{V}O_2$ data, of the three models, across three intensities: 75% of lactate threshold (θ_{LT}) (A, D, G, J), 85% θ_{LT} (B, E, H, K) and $\Delta 15\% \theta_{LT} - \dot{V}O_{2max}$ (15% of the difference between θ_{LT} and $\dot{V}O_{2max}$) (C, F, I, L). Each graph compared predicted- $\dot{V}O_2$ determined by exponential model (MRT_{EXP}) (A, B, C), linear model (MRT_{LIN}) (D, E, F), steady-state model (MRT_{SS}) (G, H, I), and no model used (NO_{MRT}) (J, K, L) to the actual $\dot{V}O_2$ determined from the last 5 min of each 30 min trial ($\dot{V}O_2$ measured). * Indicates a significant difference of $P < 0.05$

2.4 « Discussion »

This study compared three methods of ramp-incremental exercise MRT estimation to assess each method's accuracy for predicting the steady-state $\dot{V}O_2$ at constant power outputs below and slightly above θ_{LT} . The main findings were that: i) MRT_{SS} was similar to MRT_{LIN} and MRT_{EXP} , however MRT_{LIN} and MRT_{EXP} were different; ii) all models exhibited excellent accuracy for predicting steady-state $\dot{V}O_2$ response below θ_{LT} ; and iii) above θ_{LT} , MRT_{LIN} and MRT_{SS} corrections consistently underestimated the $\dot{V}O_2$ at power outputs performed in the heavy-intensity domain.

Without MRT correction, linear interpolation of the $\dot{V}O_2$ versus power output relationship from ramp-incremental exercise (i.e., NO_{MRT}) consistently underestimated the steady-state $\dot{V}O_2$ at power outputs in both the moderate- and heavy-intensity domains. The degree to which predictions fell below the actual measured steady-state $\dot{V}O_2$ response increased from a mean $-167 \text{ mL}\cdot\text{min}^{-1}$ at $75\% \theta_{LT}$, to $-217 \text{ mL}\cdot\text{min}^{-1}$ at $85\% \theta_{LT}$, and $-392 \text{ mL}\cdot\text{min}^{-1}$ at $\Delta 15$. This result demonstrates that if an MRT correction is not applied to the ramp $\dot{V}O_2$ data, then the steady-state $\dot{V}O_2$ achieved at target PO will be higher than predicted. This error will also increase as exercise intensity increases, leading to a greater underestimation of $\dot{V}O_2$ for a given power output (Figure 9). Then, to establish a good representation of the steady-state $\dot{V}O_2$ versus constant-power output relationship from ramp-incremental exercise, the MRT needs to be calculated and applied in the aerobic exercise prescription process.

2.4.2 MRT Comparisons

On average our MRT values were ~ 40 s with a range 12 s, from a minimum of 33 to a maximum of 45 s, which is similar to what other studies have observed (Boone and Bourgois 2012; Caen et al. 2020; Iannetta et al. 2019b; Keir et al. 2016a). There was no difference between MRT_{EXP} (45s) and MRT_{SS} (42 s). Furthermore, there was no difference between MRT_{LIN} (33 s) and MRT_{SS} (42 s). As such, MRT_{SS} can be considered comparable to both MRT_{EXP} and MRT_{LIN} . However, there was a significant difference between MRT_{EXP} and MRT_{LIN} . This contrasts with Iannetta et al. (2019b) who observed no differences in MRT between MRT_{EXP} , MRT_{LIN} , and the MRT_{SS} models. The difference between these findings may be attributed to differences in the study sample. For example, in their study, six of 12 participants had MRT_{EXP} and MRT_{LIN} values that were near zero.

They suggested that an MRT of zero was physiologically impossible, as this would signify that muscle $\dot{V}O_2$ is immediately reflected in the expired air with no transit delay (Iannetta et al. 2019b). This result increases the variance within participants which would reduce the probability of detecting a statistical difference (Steinberg 2012) which may account for their differential findings compared to the present study. Similarly, using nine healthy males, Caen et al. (2020) observed no difference in MRT_{LIN} and MRT_{SS} . Given the MRT comparisons observed in other studies and the ones observed in our study, MRT_{SS} can be considered comparable to both MRT_{EXP} and MRT_{LIN} . The simplicity of the MRT_{SS} determination suggests this to be the most efficacious method. Furthermore, this model is derived from the actual data collected (i.e., $\dot{V}O_2$ responses), whereas the regression models (MRT_{EXP} and MRT_{LIN}) are calculated, suggesting the MRT_{SS} to be a better reflection of an individual's actual MRT.

2.4.3 Accuracy of the Prediction Models

Within the moderate-intensity domain, all three methods of $\dot{V}O_2$ predictions were not different from the measured $\dot{V}O_2$. These results suggest that below threshold, any of the correction models may be used to accurately predict $\dot{V}O_2$ at a given power output. However, within the heavy-intensity domain, MRT_{LIN} and the MRT_{SS} underestimated the measured $\dot{V}O_2$ whereas the MRT_{EXP} -predicted $\dot{V}O_2$ was not different from the measured $\dot{V}O_2$ at this supra-threshold intensity (Table 3). It should be noted that the range of our MRT_{EXP} data of this exponential model is greater than the other predictive methods: MRT_{EXP} has a range of $1610 \text{ mL}\cdot\text{min}^{-1}$, compared to $1120 \text{ mL}\cdot\text{min}^{-1}$, $1082 \text{ mL}\cdot\text{min}^{-1}$; MRT_{LIN} and MRT_{SS} respectively (Table 3). Subsequently, this variance within the response would reduce the probability of there being a statistical difference (Steinberg 2012). In line with our findings, observing only MRT_{LIN} and MRT_{SS} , Caen et al. (2020) also showed similarities when comparing their predictive accuracy in the moderate-intensity domain. Moreover, as shown in the present paper, as exercise intensity increases the gap between the model-predicted $\dot{V}O_2$ and measured $\dot{V}O_2$ widens (Table 3). Keir et al. (2018), presented a conceptual model suggesting that this gap between constant-power output and ramp incremental $\dot{V}O_2$ continues in a nonlinear pattern up to, and past the θ_{LT} . This model also formed the basis of the research done by Caen et al. (2020), who concluded that a linear response in the dissociation between $\dot{V}O_2$ and power output was more appropriate than an exponential regression in the heavy intensity domain. The observed response in the present study from the MRT_{LIN} , MRT_{SS} , and

$\dot{V}O_{2MRT}$ -predicted $\dot{V}O_2$ supports this hypothesis, demonstrating that these two correction methods will underestimate the $\dot{V}O_2$ at intensities above θ_{LT} .

This disconnect between $\dot{V}O_2$ and the power output when $>\theta_{LT}$ which is related to the development of the $\dot{V}O_2$ slow component, has been linked to the increased oxygen cost per watt of work at these intensities (Barstow et al. 1993; Özyener et al. 2001). Previous authors have suggested that this $\dot{V}O_2$ slow component results from the exhaustion of some of the active muscle fibers at these $>\theta_{LT}$ intensities, resulting in changes in fiber recruitment patterns (Jones et al. 2011). Individual variability of the $\dot{V}O_2$ slow component is also a factor, as exhibited in figure 9L. This confounds the determination of the $\dot{V}O_2$ above the lactate threshold. This slow component related disconnect between $\dot{V}O_2$ and power output has also been observed by Caen et al. (2020), who, similarly concluded that use of the MRT_{LIN} and MRT_{SS} corrections were inappropriate at $>\theta_{LT}$ intensities, and that additional corrections were necessary if the aim was to prescribe exercise intensities from the $\dot{V}O_2$ to PO relationship observed from a ramp incremental test. Therefore, although the MRT correction is an effective method to correct the dissociation between $\dot{V}O_2$ and PO responses during ramp incremental tests within the moderate exercise intensity domain, this approach is insufficient in predicting $\dot{V}O_2$ for a given power output above the lactate threshold. This will result in steady state $\dot{V}O_2$ values for a given power output derived from the ramp incremental test that will always be greater than predicted, as the MRT cannot account for the slow component. In order to account for the $\dot{V}O_{2sc}$ during ramp incremental testing, recent publications have proposed different approaches that will contribute to making the necessary corrections (Caen et al. 2020).

2.4.4 Summary and Conclusion

This study compared the MRT and predicted $\dot{V}O_2$ accuracy of three approaches to quantify the MRT (MRT_{EXP} , MRT_{LIN} , MRT_{SS}) at intensities below (75% and 85% θ_{LT}) and above ($\Delta 15$) lactate threshold. While in clinical settings researchers have used heart rate (HR) to prescribe exercise intensity, there is a lack of consensus on the appropriate ranges used to define exercise intensity categories due to large individual variability of HR (Tran et al. 2022). Furthermore, the inability of HR to attain a steady-state response at any intensity during CPE (cardiac drift) reduces the precision of exercise prescription when using %HRmax (Iannetta et al. 2020). As such, it is optimal to use ventilatory thresholds and $\dot{V}O_2$ -based MRT corrections during ramp incremental exercise

to prescribe accurate exercise intensity. Considering the benefits and limitations of each model, and the findings presented in this study, we suggest the use of MRT_{SS} . It is a simple method that is not susceptible to the same issues as other fitting models, provides greater reliability, and provides an MRT estimate that is comparable to both MRT_{EXP} and MRT_{LIN} . Moreover, our observations further strengthen the recommendation that a MRT correction method must be used to ensure appropriate exercise prescription when deriving exercise intensities within the moderate intensity domain from ramp incremental tests.

2.4.5 Limitations and Future Directions

This study collected data from participants with different fitness levels ranging from recreationally active to well-trained individuals. Since a large portion of the general population is considered sedentary, it would have been more applicable to include sedentary individuals to better reflect the state of the general population. Furthermore, female participants should be included in future studies to evaluate sex differences in MRT and correction models' accuracies. Research has shown that exercise performance is affected during different menstrual cycle phases, particularly the early follicular phase (McNulty et al. 2020). Also, De Poli et al (2019) observed that men presented a greater anaerobic capacity than women. This difference in metabolic activity may contribute to a difference in MRT values. As such, potential studies should look to observe the impact of these sex differences on the MRT. Further research is also required to better understand the relationship between PO and the $\dot{V}O_2$ response, especially above the lactate threshold. Future studies may focus on the mathematical relationship between these physiological changes and attempt to define a MRT correction model that can take these into consideration without further complicating or lengthening the protocol.

2.5 « References »

- Bailey SJ, Romer LM, Kelly J, Wilkerson DP, DiMenna FJ, Jones AM (2010) Inspiratory Muscle Training Enhances Pulmonary O₂ Uptake Kinetics And High-Intensity Exercise Tolerance In Humans. *Journal Of Applied Physiology* (Bethesda, Md: 1985) 109:457–68. <https://doi.org/10.1152/jappphysiol.00077.2010>
- Barstow TJ, Casaburi R, Wasserman K (1993) O₂ Uptake Kinetics And The O₂ Deficit As Related To Exercise Intensity And Blood Lactate. *Journal Of Applied Physiology* 75:755–762. <https://doi.org/10.1152/jappl.1993.75.2.755>
- Boone J, Bourgois J (2012) The Oxygen Uptake Response To Incremental Ramp Exercise. *Sports Medicine* 42:511–526. <https://doi.org/10.2165/11599690-000000000-00000>
- Caen K, Boone J, Bourgois JG, Colosio AL, Pogliaghi S (2020) Translating Ramp $\dot{V}O_2$ Into Constant Power Output: A Novel Strategy That Minds The Gap. *Medicine & Science In Sports & Exercise* 52:2020–2028. <https://doi.org/10.1249/Mss.0000000000002328>
- De Poli RA, Gonzalez JAM, Fonsati N, Zagatto AM (2019). Differences Between Genders in Anaerobic Capacity During a Supramaximal Effort. *Motriz: Revista De Educação Física*, 25(3). <https://doi.org/10.1590/s1980-6574201900030018>
- Grey TM, Spencer MD, Belfry GR, Kowalchuk JM, Paterson DH, Murias JM. (2015). Effects of age and long-term endurance training on $\dot{V}O_2$ kinetics. *Medicine and science in sports and exercise*, 47(2), 289–298. <https://doi.org/10.1249/MSS.0000000000000398>
- Iannetta D, De Almeida Azevedo R, Keir DA, Murias JM (2019a) Establishing The $\dot{V}O_2$ Versus Constant-Work-Rate Relationship From Ramp-Incremental Exercise: Simple Strategies For An Unsolved Problem. *Journal Of Applied Physiology* 127:1519–1527. <https://doi.org/10.1152/jappphysiol.00508.2019>
- Iannetta, D., Inglis, E. C., Mattu, A. T., Fontana, F. F., Pogliaghi, S., Keir, D. A., Murias, J. M. (2020). A Critical Evaluation Of Current Methods For Exercise Prescription in Women

and Men. *Medicine & Science in Sports & Exercise*, 52(2), 466–473.
<https://doi.org/10.1249/mss.0000000000002147>

Iannetta D, Murias JM, Keir DA (2019b) A Simple Method To Quantify The $\dot{V}O_2$ Mean Response Time Of Ramp-Incremental Exercise. *Medicine & Science In Sports & Exercise* 51:1080–1086. <https://doi.org/10.1249/Mss.0000000000001880>

Jones AM, Grassi B, Christensen PM, Krstrup P, Bangsbo J, Poole DC (2011) Slow Component Of $\dot{V}O_2$ Kinetics: Mechanistic Bases And Practical Applications. *Medicine And Science In Sports And Exercise* 43:2046–62.
<https://doi.org/10.1249/MSS.0b013e31821fcfc1>

Keir DA, Benson AP, Love LK, Robertson TC, Rossiter HB, Kowalchuk JM (2016) Influence Of Muscle Metabolic Heterogeneity In Determining The $\dot{V}O_{2p}$ Kinetic Response To Ramp-Incremental Exercise. *Journal Of Applied Physiology (Bethesda, Md: 1985)* 120:503–513. <https://doi.org/10.1152/Jappphysiol.00804.2015>

Keir DA, Iannetta D, Mattioni Maturana F, Kowalchuk JM, Murias JM (2021) Identification Of Non-Invasive Exercise Thresholds: Methods, Strategies, And An Online App. *Sports Medicine* 52:237–255. <https://doi.org/10.1007/S40279-021-01581-Z>

Keir DA, Paterson DH, Kowalchuk JM, Murias JM (2018) Using Ramp-Incremental $\dot{V}O_2$ Responses For Constant-Intensity Exercise Selection. *Applied Physiology, Nutrition, And Metabolism* 43:882–892. <https://doi.org/10.1139/Apnm-2017-0826>

Keir DA, Robertson TC, Benson AP, Rossiter HB, Kowalchuk JM (2015) The Influence Of Metabolic And Circulatory Heterogeneity On The Expression Of Pulmonary Oxygen Uptake Kinetics In Humans. *Experimental Physiology* 101:176–192.
<https://doi.org/10.1113/Ep085338>

McKay AKA, Stellingwerff T, Smith ES, Martin DT, Mujika I, Goosey-Tolfrey VL, Sheppard J, Burke LM (2022) Defining Training And Performance Caliber: A Participant Classification Framework. *International Journal Of Sports Physiology And Performance* 17:1–15. <https://doi.org/10.1123/Ijspp.2021-0451>

- McNulty, K. L., Elliott-Sale, K. J., Dolan, E., Swinton, P. A., Ansdell, P., Goodall, S., Thomas, K., & Hicks, K. M. (2020). The Effects of Menstrual Cycle Phase on Exercise Performance in Eumenorrhic Women: A Systematic Review and Meta-Analysis. *Sports medicine* 50(10), 1813–1827. <https://doi.org/10.1007/s40279-020-01319-3>
- Özyener F, Rossiter HB, Ward SA, Whipp BJ (2001) Influence Of Exercise Intensity On The On- And Off-Transient Kinetics Of Pulmonary Oxygen Uptake In Humans. *The Journal Of Physiology* 533:891–902. <https://doi.org/10.1111/J.1469-7793.2001.T01-1-00891.X>
- Pescatello LS, American College Of Sports Medicine (2014) ACSM’s Guidelines For Exercise Testing And Prescription. Wolters Kluwer/Lippincott Williams & Wilkins Health, Philadelphia
- Spencer MD, Murias JM, Kowalchuk JM, Paterson DH (2012) Effect Of Moderate-Intensity Work Rate Increment On Phase II $\dot{V}O_2$, Functional Gain And $\Delta[Hbb]$. *European Journal Of Applied Physiology* 113:545–557. <https://doi.org/10.1007/S00421-012-2460-3>
- Steinberg WJ (2012) *Statistics Alive!* 2nd Edn. Sage Publications
- Swanson GD, Hughson RL (1988) On The Modeling And Interpretation Of Oxygen Uptake Kinetics From Ramp Work Rate Tests. *Journal Of Applied Physiology* 65:2453–2458. <https://doi.org/10.1152/Jappl.1988.65.6.2453>
- Tran DL, Kamaladasa Y, Munoz PA, Kotchetkova I, D'Souza M, Celermajer DS, Maiorana A, Cordina R (2022). Estimating Exercise Intensity Using Heart Rate In Adolescents And Adults With Congenital Heart Disease: Are Established Methods Valid? *International Journal Of Cardiology Congenital Heart Disease*, 8, 100362. <https://doi.org/10.1016/j.ijcchd.2022.100362>
- Whipp BJ, Davis JA, Torres F, Wasserman K (1981) A Test To Determine Parameters Of Aerobic Function During Exercise. *Journal Of Applied Physiology* 50:217–221. <https://doi.org/10.1152/Jappl.1981.50.1.217>

Whipp BJ, Ward SA, Lamarra N, Davis JA, Wasserman K (1982) Parameters Of Ventilatory And Gas Exchange Dynamics During Exercise. *Journal Of Applied Physiology* 52:1506–1513. <https://doi.org/10.1152/jappl.1982.52.6.1506>

Wilcox SL, Broxterman RM, Barstow TJ (2016) Constructing Quasi-Linear $\dot{V}O_2$ Responses From Nonlinear Parameters. *Journal Of Applied Physiology* 120:121–129. <https://doi.org/10.1152/jappphysiol.00507.2015>

Appendix

Ethics Approval Notice



Date: 12 July 2019

To: Dr. Glen Belfry

Project ID: 114222

Study Title: Are constant load training intensities predictable from the VO2 response of a Ramp Test?

Application Type: HSREB Initial Application

Review Type: Full Board

Meeting Date: 02/Jul/2019 13:00

Date Approval Issued: 12/Jul/2019 15:09

REB Approval Expiry Date: 12/Jul/2020

Dear Dr. Glen Belfry

The Western University Health Science Research Ethics Board (HSREB) has reviewed and approved the above mentioned study as described in the WREM application form, as of the HSREB Initial Approval Date noted above. This research study is to be conducted by the investigator noted above. All other required institutional approvals must also be obtained prior to the conduct of the study.

Documents Approved:

Document Name	Document Type	Document Date	Document Version
Advertisement_Jul8_clean	Recruitment Materials	08/Jul/2019	
Data Collection	Other Data Collection Instruments	08/Jul/2019	1
Letter of Information and Consent_July 10_2019_clean	Written Consent/Assent	10/Jul/2019	3
Methods	Protocol	08/Jul/2019	
ParQ,GAQ_CSEPPATH Readines Form	Other Data Collection Instruments	10/Jul/2019	3

No deviations from, or changes to, the protocol or WREM application should be initiated without prior written approval of an appropriate amendment from Western HSREB, except when necessary to eliminate immediate hazard(s) to study participants or when the change(s) involves only administrative or logistical aspects of the trial.

REB members involved in the research project do not participate in the review, discussion or decision.

The Western University HSREB operates in compliance with, and is constituted in accordance with, the requirements of the TriCouncil Policy Statement: Ethical Conduct for Research Involving Humans (1CPS 2); the International Conference on Harmonisation Good Clinical Practice Consolidated Guideline (ICH GCP); Part C, Division 5 of the Food and Drug Regulations; Part 4 of the Natural Health Products Regulations; Part 3 of the Medical Devices Regulations and the provisions of the Ontario Personal Health Information Protection Act (PHIPA 2004) and its applicable regulations. The HSREB is registered with the U.S. Department of Health & Human Services under the IRB registration number IRB 00000940.

Please do not hesitate to contact us if you have any questions.

Sincerely,

Nicola Geoghegan-Morphet, Ethics Officer on behalf of Dr. Joseph Gilbert, HSREB Chair

Note: This correspondence includes an electronic signature (validation and approval via an online system that is compliant with all regulations).

Curriculum Vitae

Name: Nikan Behboodpour

**Post-secondary
Education and
Degrees:** Western University
London, Ontario, Canada
2016-2020 B.A.

The University of Western Ontario
London, Ontario, Canada
2020-2023 M.Sc.

**Related Work
Experience** Teaching Assistant
The University of Western Ontario
2020-2022

Patient Care Coordinator
Mackenzie Spine and Brain Associates
2022-2023

Publications: Tari, B., Shirzad, M., Behboodpour, N., Belfry, G. R., & Heath, M.
(2021). Exercise intensity-specific changes to cerebral blood velocity do
not modulate a post-exercise executive function benefit.
Neuropsychologia, 161, 108018.

**Conference
Presentations
& Posters** Behboodpour, N., Keir, D., Halvorson, B., Belfry, G., Comparison of
Different Methods Used to Prescribe Exercise Intensities From Ramp-
Incremental Exercise: 123 (2022). *Medicine & Science in Sports &
Exercise* 54(9S): p 21-22. DOI: 10.1249/01.mss.0000875320.88723.46